

See discussions, stats, and author profiles for this publication at: <https://www.researchgate.net/publication/353971086>

# A Comprehensive Review on CubeSat Electrical Power System Architectures

Article in IEEE Transactions on Power Electronics · August 2021

DOI: 10.1109/TPEL.2021.3110002

---

CITATIONS

36

READS

2,349

---

6 authors, including:



Amarendra Edpuganti

Indian Institute of Technology Kanpur

40 PUBLICATIONS 1,032 CITATIONS

[SEE PROFILE](#)



Vinod Khadkikar

Khalifa University

63 PUBLICATIONS 715 CITATIONS

[SEE PROFILE](#)



M.s. El Moursi

Khalifa University of Science and Technology - Masdar Campus

269 PUBLICATIONS 7,443 CITATIONS

[SEE PROFILE](#)

# A Comprehensive Review on CubeSat Electrical Power System Architectures

Amarendra Edpuganti, *Member, IEEE*, Vinod Khadkikar, *Senior Member, IEEE*,  
 Mohamed Shawky El Moursi, *Senior Member, IEEE*, Hatem Zeineldin, *Senior Member, IEEE*,  
 Naji Al Sayari, and Khalifa Al Hosani, *Senior Member, IEEE*

**Abstract**—CubeSats have been popular for space research due to lower cost, faster development, and easier deployment. The electrical power system (EPS) is one of the significant subsystem for the CubeSat since it handles power generation, energy storage, and power distribution to all other subsystems. Therefore, the design of EPS becomes crucial for successful CubeSat mission, wherein the first step is the selection of EPS architecture. The main objective of this paper is to present an extensive review of all the conventional and emerging EPS architectures of CubeSats. A total of seventeen categories of CubeSat EPS architectures have been identified, classified, and the operational aspects of these architectures are presented in addition to a qualitative comparison. This study is expected to provide a useful reference guide for all the researchers and developers working in the area of CubeSats EPS. Also, some of the potential research topics are provided to further exploration and innovation for the CubeSat EPS.

**Index Terms**—CubeSat, Electrical power system, Nanosatellites, DC-DC converters, Low-earth-orbit (LEO) satellites.

## I. INTRODUCTION

**D**EVELOPMENT of advanced electronics have enabled building of CubeSats with powerful capabilities that were previously dominated by larger satellites. CubeSat belongs to the category of nanosatellite which is built in multiples of 1U ( $10 \times 10 \times 10 \text{ cm}^3$ ) units. The CubeSat standards were originally proposed to enable students to learn, design, and test them in space [1], [2]. The concept of CubeSats gave affordable access to low-budget research programs for an ever increasing space missions to perform scientific experiments and validate new space technologies [3]. The very first set of six CubeSats were

Manuscript received March 02, 2021; revised July 07, 2021; accepted August 18, 2021. This work was supported by Advanced Power & Energy center (APEC) at Khalifa University. (Corresponding author: Vinod Khadkikar.)

Amarendra Edpuganti, Naji Al-Sayari, and Khalifa Al Hosani are with Advanced Power & Energy Center (APEC), Electrical Engineering and Computer Science Department, Khalifa University, Abu Dhabi 127788, UAE (e-mail: amarendra.edpuganti@ku.ac.ae, naji.alsayari@ku.ac.ae, khalifa.halhosani@ku.ac.ae).

Vinod Khadkikar is with the Advanced Power & Energy (APEC) and Khalifa University Space Technology & Innovation (KUSTIC) centers, Electrical Engineering and Computer Science Department, Khalifa University, Abu Dhabi 127788, UAE (e-mail: vinod.khadkikar@ku.ac.ae).

Mohamed Shawky El Moursi is with Advanced Power & Energy Center (APEC), Electrical Engineering and Computer Science Department, Khalifa University, Abu Dhabi 127788, UAE (e-mail: mohamed.elmoursi@ku.ac.ae). M.S. El Moursi is currently on leave from the Faculty of Engineering, Mansoura University, Mansoura 35516, Egypt.

H. H. Zeineldin is with Advanced Power & Energy Center (APEC), Khalifa University, UAE and is currently on leave from the Faculty of Engineering, Cairo University, Giza, Egypt (e-mail: hatem.zeineldin@ku.ac.ae).

Color versions of one or more of the figures in this article are available online at <https://ieeexplore.ieee.org>.

Digital Object Identifier 10.1109/TPEL.2021.xxxxx

launched on June 30, 2003 on Eurockot [4] and since then, more than 1300 CubeSats have been launched [5]. Initially, academic institutes had majority of CubeSat launches, whereas most of the recent CubeSat launches are done for commercial purposes. The details of all the CubeSats that are launched as well as in planning stage can be seen in [5], [6]. The list of some of the academic CubeSats referred in this paper are shown in Table I.

The CubeSats are usually launched in low earth orbit (LEO) which is an Earth-centered orbit with an altitude of 2000 km or less and an orbit period of 90 to 120 minutes [7]. The LEO CubeSat's orbit can have inclination angle from 0 to 98 degrees with respect to equatorial plane. They are visible to a Earth station for a few minutes in every orbit. As the CubeSat revolves in an orbit, it experiences both sunlit and eclipse periods. In sunlit period, the CubeSat is illuminated by sunlight and the angle of incidence of sunlight on the photovoltaic (PV) arrays varies from 66.55 to 90 degrees. During eclipse period, the Earth blocks the sunlight from illuminating the CubeSat once in every orbit in all seasons and the temperature drops

TABLE I  
LIST OF SOME ACADEMIC CUBESETS

Name	Size	University	Launch Year
CanX-1	1U	University of Toronto	2003
QuakeSat	3U	Stanford University	2003
CUTE-1	1U	Tokyo Institute of Technology	2003
NCube-1	1U	NTNU	2006
GeneSat-1	3U	Santa Clara University	2006
MEROPE	1U	Montana State University	2006
Cute-1.7+APD	2U	Tokyo Institute of Technology	2006
PicPot	2U	Polytechnic Univ. of Turin	2006
Goliat	1U	University of Bucharest	2012
ESTCube-1	1U	University of Tartu	2013
LituaniaSAT-1	1U	Kaunas Univ. Tech.	2014
Aoxiang-Sat	12U	Northwestern Poly. Univ.	2016
Swayam	1U	College of Engineering, Pune	2016
OUFTI-1	1U	University of Liege	2016
KySat-2	1U	University of Kentucky	2017
CP1	3U	California Poly. State Univ.	2018
Zacube-2	3U	Cape Peninsula Univ. Tech.	2018
MYSAT-1	1U	Khalifa University	2018
FloripaSat1	1U	Federal Univ. of Santa Catarina	2019
TTUSat	1U	Tallinn University of Technology	2019
PR-CuNaR2	3U	Inter American Univ. Puerto Rico	2021
Liberdad-2	3U	Sergio Arboleda University	2021
NutSat	2U	National Formosa University	2021
RVSAT-1	2U	R V College of Engineering	2022
PilsenCube2	1U	Univ. West Bohemia	2023

sharply. The eclipse period is dependent on the orbit altitude, inclination, and the sunlight incidence angle on the orbit plane known as  $\beta$  angle [7]. The eclipse duration is longest at  $\beta = 0$  and as  $\beta$  increases the eclipse duration decreases up to the point of no eclipse, for example, polar orbits never have eclipse period. A typical LEO CubeSat has an eclipse period for 1/3 of the orbit period [8]. The calculation of eclipse period is important in the design of CubeSat EPS especially the storage system. Recently, with the successful launch to Mars orbit, CubeSats are being actively explored beyond LEO missions [9]–[11].

The main subsystems of the CubeSat are as follows: electrical power system (EPS), on-board computer (OBC), attitude determination and control system (ADCS), command and data handling system (CDH), communication receiver (COM RX), and communication transmitter (COM TX). One of the challenges in the CubeSats is to ensure that all subsystems fit within a limited budget of volume and weight. In addition, all the subsystems should be tolerant to severe radiation, wide range of temperature, and should be highly reliable as there is no possibility of maintenance after launch [12]. In LEO, typical temperature range of solar cells are from -100 to 100°C, whereas the CubeSat components have typical range from -40 to 80°C [13]. The thermal control inside CubeSat is achieved by both passive and active thermal control methods [14].

The EPS is an essential subsystem of CubeSat that powers all the other subsystems. The basic components of EPS are shown in Fig. 1. It consists of PV panels as primary energy source, energy storage system, power electronic converters, and power distribution system. The sizing and arrangement of CubeSat PV panels depends on the mission specific requirements [15]. The installed capacity of the PV panels is limited by the volume and weight constraints of CubeSat.

The PV panels of CubeSat are either mounted on facets or deployable or combination of both [16]. The total amount of solar power generation in an orbit depends on the incidence angle of sunlight on the PV panels, and arrangement of PV panels (fixed or deployable) [17], [18]. The ADCS determines the total amount of power generation by controlling the CubeSat in three different operational modes : nadir-pointing, full Sun-tracking, and partial Sun-tracking [19]. The full and partial Sun-tracking modes are possible in CubeSats with the deployable panels [16]. In the full sun-tracking mode, the PV panels are oriented towards the sun to maximize the solar power generation [20]. However, this operational mode may not be used continuously as it affects the performance and data collection from the payloads. Therefore, the partial Sun-tracking mode is used in which the CubeSat is oriented within

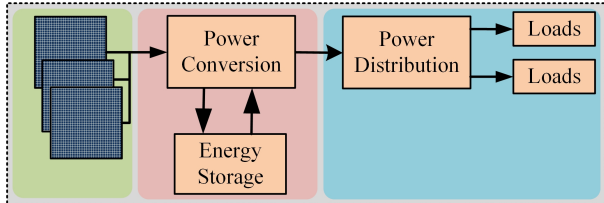


Fig. 1. Basic components of CubeSat EPS.

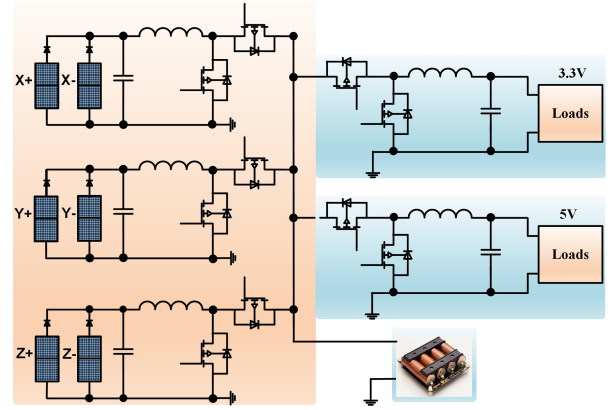


Fig. 2. Typical commercial EPS architecture of CubeSats [27]–[31].

10 degrees off-nadir [21]. In this mode, the amount of power generation is higher than nadir-pointing mode but less than full Sun-tracking mode. In the nadir-pointing mode, the CubeSat is oriented towards the Earth.

The storage system is required during eclipse period and peak load conditions. The energy storage system consists of lithium-ion (Li-ion) cells due to higher energy density, higher number of charge/discharge cycles, and lower self-discharge rate [22]. On the other hand, the Li-ion batteries have following disadvantages: (1) the life-cycle of Li-ion battery degrades due to higher charge/discharge rates [23], (2) Li-ion battery has limited energy density at lower temperatures ( $< -20^{\circ}\text{C}$ ), and (3) Charge rate of Li-ion battery is very low at lower temperatures with the possibility of life reduction [24]. This leads to performance issues in deep space as well as low-duty cycle high power applications in LEO such as synthetic-aperture radar. Therefore, CubeSats have been using ultracapacitor (UC) [25] or hybrid energy storage which combines both UC and battery [26] in order to achieve high power density, higher reliability, and better performance at lower temperatures. A battery heater circuit is also used in EPS to keep the batteries temperature in the recommended operational range.

A typical commercial off-the-shelf (COTS) EPS architecture for a fixed panel CubeSat is shown in Fig. 2 [27]–[31]. On the generation-side, the PV panels on the opposite facets of CubeSat are connected in parallel and they are interfaced with dc-dc converter for maximum power point tracking (MPPT) under wide range of irradiation conditions and battery voltage. The type of dc-dc converter depends on the maximum power point (MPP) voltage of the PV panel and the battery voltage. In general, synchronous buck or boost or buck-boost topologies are used to achieve highly efficient power conversion. The Each PV panel will have series diode to prevent non-illuminated panels from drawing power from the sunlit panels. The output of MPPT converters is connected in parallel across battery terminals and this dc-bus voltage is further distributed to all other subsystems and payloads. Most of the subsystems and payloads usually require voltage regulators for their operation.

In the literature, researchers presented the mission specific details of CubeSat EPS and high-level comparison between the different EPS architectures [32]–[35]. In [32], direct energy

transfer (DET) and peak power transfer (PPT) architectures are compared with respect to reliability. In [33], the comparison is done in terms of overall mass while considering total power margin in a full orbit. In [34], an overall performance index is defined based on efficiency, reliability, and cost, and then the comparison is done between DET and PPT architectures. In [35], the comparison between different PPT architectures is done in terms of orbital efficiency for all operating modes, component count, reliability, and battery size, while considering the real data of a CubeSat.

The main objective of this paper is to present extensive review of all the existing EPS architectures [27]–[31], [36]–[95], classify them in different categories, present the operational details, and perform qualitative comparison. This paper attempts to briefly present the details of some of the CubeSat EPS architectures based on the available information. Also, this paper aims to help the researchers to identify some of the best possible EPS architectures so that the detailed comparison studies can be done based on the mission specific requirements [35]. In addition, the paper identifies potential research topics in CubeSat EPS for further exploration and innovation.

## II. DESIGN AND ENERGY MANAGEMENT OF CUBESAT EPS

The design of CubeSat EPS starts after defining the mission specific requirements such as mission objectives, orbit parameters (e.g. altitude and inclination angle), and payload specifications [96]. The mission objectives include mission duration and goal of mission like earth observation, remote sensing, communication, performing scientific experiments, etc. The payload specifications include the power consumption and the duration of payload operation in each orbit. For example, the earth observation CubeSat need to take image of a particular location on the earth in some specific or every orbit. Also, the operation of other subsystems is planned to support the payload operation. For example, ADCS need to detumble or point the CubeSat before taking the image. The CubeSat operational modes are then defined to meet payload operational as well as all other subsystems requirements [35]. Based on all these specifications, the size of CubeSat and the arrangement of PV panels (body mount or deployable or combination of both) are determined. Once all the requirements and specifications are identified, the CubeSat developers have two options of either designing their own EPS or using the COTS EPS to meet their power budget needs.

For the first option, the EPS design starts with the selection of appropriate EPS architecture based on the comparison of overall efficiency, battery size, and reliability for the given mission specific requirements [35]. Next, the total energy that can be generated by PV panels in each orbit is calculated considering the irradiation profile of the entire mission duration. After that, the maximum load consumption in any orbit is calculated based on the operational modes of CubeSat. Then, the number of Li-ion cells ( $N_{cell}$ ) is calculated considering the minimum energy generation ( $E_{Gmin}$ ) and maximum load consumption in an orbit ( $E_{Lmax}$ ). While calculating  $N_{cell}$ , the first step is to calculate the cycle life ( $N_{cycle}$ ) considering

the mission duration. Based on  $N_{cycle}$ , values of depth-of-discharge (DOD) and end of charge voltage (EOCV) can be estimated from battery data sheet. The values of DOD and EOCV determine the available capacity of Li-ion cell and thus, the required number of cells can be calculated for the CubeSat EPS. If the battery size is more than the space allocated to EPS, the PV panel arrangement need to be changed and/or the operational modes based on the energy management.

For the COTS EPS, the operational modes have to be verified for the entire mission duration to check whether the PV panel arrangement and size of battery are sufficient to satisfy the energy requirements. If there is any scenario where the load consumption is exceeding both the generation and storage energy, the following options exists : (1) change the PV panel arrangement to increase the power generation, (2) increase the battery size in case of availability of free space, and (3) change the load profile based on the energy management to balance the energy generation and load consumption.

Finally, the energy management of CubeSat plays an important role in achieving the desired mission objectives while maintaining the appropriate power balance. It becomes crucial when the load demand exceeds the available power generation and storage. In general, the operational modes of CubeSat such as normal mode and safe mode are defined for each orbit and thus, it is easy to calculate the energy available in the battery at the end of each orbit. In the safe mode of operation (battery energy is falling below the threshold limit), all the noncritical loads are switched-off until the time where the battery is fully charged. The normal mode of operation can be several types depending on the operation of payloads and other subsystems. For example, one of the normal mode can be for taking image of a specific location and other can be for transmitting data to ground station.

To understand the energy management strategy in general, consider the case study of MYSAT-1, which is an 1U CubeSat launched by Khalifa University for earth observation and technology demonstration purpose. The payloads of MYSAT-1 consist of camera for imaging and battery for testing its performance. Apart from safe mode, the following normal operation modes are defined for MYSAT-1: (1) Imaging mode; 2) pointing or detumbling mode; 3) data download (DATA); 4) experimental battery testing (EBT); 5) experimental battery testing followed by data download (EBT+DATA). In each orbit, the subsystems OBC, EPS, and COM RX operate for entire duration, whereas the COM TX operates during beacon period for 6.4 minutes and/or during ground access time for 10.5 min. In the imaging mode, the camera remains idle for 5 min prior to taking an image and then it is made operational for 1 min to take an image. In pointing/detumbling mode, ADCS is operational for the entire orbit except during the beacon period, wherein COM TX is working. The total energy consumption for the different modes of operation are shown in Table II.

The Systems Tool Kit (STK) software is used to obtain the total power generation in each orbit for the entire mission duration of six months. The minimum and maximum values of energy generated in an orbit are calculated as 2243 mWh, and 3066 mWh, respectively. Based on Table II, it should

TABLE II  
ENERGY DEMAND FOR OPERATIONAL MODES OF MYSAT-1

Mode	Safe	Imaging	Detumbling/ Pointing	EBT	DATA	EBT+ DATA
Energy Demand (mWh)	2073	5125	4419	2251	3006	3184

be observed that both the imaging and detumbling modes demand more energy than the power generation and thus, energy management strategy should decide the frequency of their operation such that battery does not get drained.

One of the sequence of operational modes decided by energy management strategy based on the energy generation and load consumption is shown in Table III. Initially, the CubeSat operates in safe mode for 12 orbits to ensure that battery is fully charged. Then, it goes for detumbling mode for next 5 orbits and after that, it goes into data download mode for next seven orbits (17-25) to collect housekeeping data as well as to charge the battery again. However, the data download will happen only when there is access to ground station. Next, it will go into detumbling mode for next five orbits (26-30) and data download mode for seven orbits (31-37). Next, the CubeSat goes into pointing/detumbling (38-40) mode before taking image in 41<sup>st</sup> orbit. Also, the experimental battery testing is done in orbits (53-55), which is the secondary payload of the mission and it will continue for more orbits depending on the number of cycles of charging/discharging required. It should be highlighted that the energy management strategy is simpler for CubeSats due to availability of power generation data and flexibility in planning operational modes. Another aspect of energy management strategy is to ensure that the initial charging level of battery should balance the power generation and load consumption in the first orbit. More details about the design, control, and power management of CubeSat EPS can be seen found in [93], [96].

### III. CLASSIFICATION OF CUBESAT EPS ARCHITECTURES

The EPS design is critical for CubeSat mission success wherein selection of EPS architecture is one of the important step [96]. The classification of the state-of-the-art CubeSat EPS architectures is shown in Fig. 3, which is done based on the following aspects: (1) dc-bus voltage regulation, (2) interface of PV panels, (3) location of power converters, and (4) number of conversion stages.

TABLE III  
SEQUENCE OF OPERATIONAL MODES FOR MYSAT-1

Mode	Orbits	Mode	Orbits
Safe Mode	1-12	Imaging	41
Detumbling	14-18	DATA	42-48
DATA	17-25	Pointing	49-51
Detumbling	26-30	Imaging	52
DATA	31-37	EBT	53-54
Pointing	38-40	EBT+DATA	55

#### A. Dc-bus Voltage Regulation

The dc-bus acts as intermediate stage between PV panels, energy storage system, and loads. Based on the dc-bus voltage regulation, the EPS architectures are classified as: (1) unregulated dc-bus EPS [27]–[31], [36]–[88], (2) regulated dc-bus EPS [38], [77], [89]–[94], and (3) sun-regulated dc-bus EPS [7], [89], [95]. The unregulated dc-bus EPS has battery terminals connected to dc-bus and it is most popular in COTS EPS [27]–[31]. In case of the regulated dc-bus, a dedicated dc-dc converter is used to regulate the bus voltage close to reference value. In sun-regulated dc-bus architecture, the dc-bus voltage is regulated to reference value only during the sunlit period and during the eclipse period, the battery connects to the dc-bus via diode. It is also referred as partial regulated dc-bus or quasi regulated dc-bus in the literature [7].

#### B. Interface of PV Panels

The PV panels are the main source of energy for the CubeSats and based on their interface, the EPS architectures are categorized into DET and PPT [94].

1) *DET architecture*: In this architecture, the PV panels with series diodes are directly connected to storage system and/or loads [7], [36]–[45], [89]. It usually has a shunt regulator in parallel to the PV panel to divert the excess PV power when the battery is fully charged or when the load demand is less. The excess power is dissipated as heat inside CubeSat if resistor is used in shunt regulator otherwise it is dissipated on the PV panel. The reliability of shunt regulator is very important otherwise it results in loss of mission. It provides simplest and cheapest solution with reduced parts count and consequently, higher reliability in radiation environment. The main drawback of this configuration is the under utilization of PV panel generation capacity which is crucial for CubeSats due to limited power generation and storage capacity.

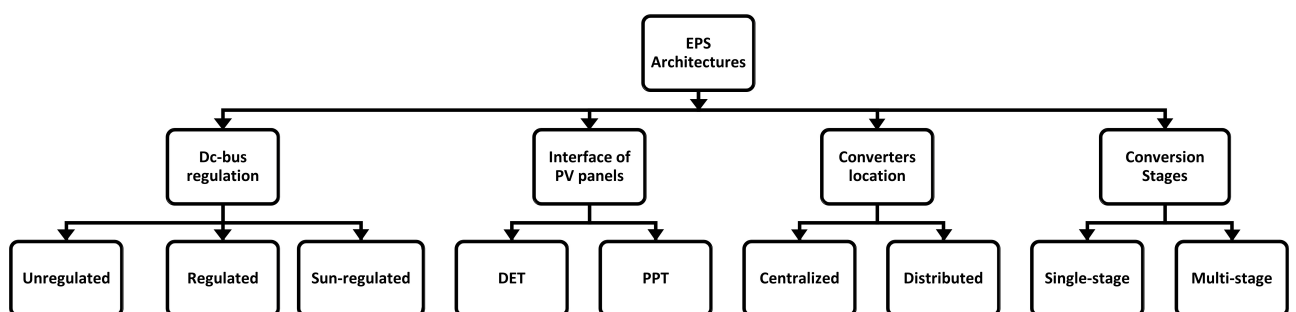


Fig. 3. Classification of CubeSat EPS architectures.

2) *PPT architecture*: The architecture utilizes PV panels interfaced with dc-dc converters as shown in Fig. 2 to achieve MPPT over wide range of operating conditions such as solar irradiation, PV panel temperature, and sun inclination angle [27]–[31], [38], [46]–[77], [77]–[79], [79]–[88], [90]–[95]. It is widely used in CubeSat designs as they have limited power generation due to shorter sunlit periods and space constraints for using larger PV panels [27]–[31]. The MPPT can be achieved by either digital micro-controller (MCU) [] or analog controllers [53], [62], [63]. A MCU has advantages of simplicity and flexibility in tuning but it is more susceptible to failure due to radiation damage. The analog controller with discrete components is considered more robust although not efficient as MCU. The CubeSats may implement analog controllers as main control [62], [63] or as back-up control to be used in case of MCU failure [53]. In [69], EPS utilized both DET and PPT architectures due to different sized PV arrays. The MPPT converter is used on a panel which had different size than other panels so that it operates at same voltage as other larger PV panels . In another CubeSat, DET is used for some of the PV panels which feeds to Li-ion batteries and PPT is used for remaining panels to supply solar power to UC [38].

### C. Location of Power Converters

Based on the location of power converters, the EPS architectures are categorized as centralized/concentrated and decentralized/distributed architectures as shown in Fig. 4.

1) *Centralized architecture*: In the centralized architecture of Fig. 4 (a), all the power converters along with the controllers are placed on a single printed circuit board (PCB) which connects to the PV modules, storage system, payloads, and subsystems through specific voltage rails [27]–[31], [36]–[40], [43]–[45], [48]–[51], [53]–[69], [72]–[81], [83]–[87], [90]–[93], [97]. It has been widely used in CubeSats due to

simplicity, physical space efficiency, and several COTS EPS designs [27]–[31]. In this architecture, fewer voltage regulators are required because multiple payloads and subsystems use same voltage rail. One main disadvantage is that the voltage regulators must be designed for peak load demand and hence, the converter operate at lower efficiency for most of the time. Another disadvantage is lower reliability as the failure of one converter affects multiple subsystems [38].

2) *Distributed Architecture*: The distributed architecture shown in Fig. 4 (b) has dc-bus supplied throughout the system and the power converters are placed close to individual subsystems [41], [42], [70], [89], [95] and in some designs, MPPT converters are placed close to PV panels [71], [98]. In [71], the MPPT converters are designed to be placed back of the PV panels so that freed up space on the EPS board can be used for placing redundant components. It utilizes several PCBs in the entire design and is commonly used in bigger satellites but has not become popular in CubeSats due to higher number of dedicated power converters. However, recent development of compact monolithic dc-dc converters with high efficiency have been providing the opportunities to implement distributed architectures for CubeSat. Also, the development of charge pump or switched capacitor converters (SCC) with smaller footprints facilitate adaptation of distributed architectures in CubeSats [66], [95]. The major advantages of distributed architectures are: modularity, redundancy, re-usability for multiple missions, irradiated noise reduction, flexibility, and homogeneous thermal distribution [95]. The reduction of radiation noise is due to placement of point-of-load (POL) converters close to load which reduces current loops and dc-bus coupling [89]. The better thermal distribution is due to distribution of power converters.

### D. Number of Conversion Stages

Depending on the number of power conversion stages, the EPS architectures are classified as single-stage and multi-stage [99].

1) *Single-stage Architecture*: A single-stage architecture for CubeSat EPS is shown in Fig. 5. It utilizes single conversion stage such as multiple-input-multiple-output (MIMO) converters to perform MPPT, charge/discharge regulation of battery, and voltage regulation for all the subsystems and payloads. It has lower component count, higher efficient conversion, and smaller footprint. It has higher control complexity that arises from coupling between different system variables

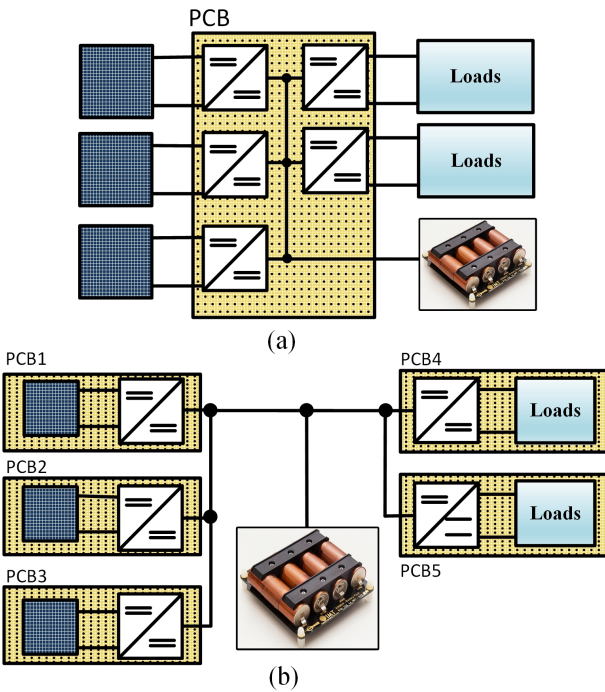


Fig. 4. Types of EPS architectures based on location of converters. (a) Centralized (b) Distributed.

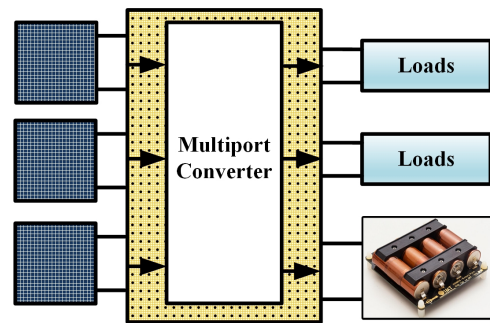


Fig. 5. Single-stage EPS architecture.

and lower performance under wide operating conditions. At this point of time, neither publications nor patents are available focusing on the single-stage architecture for CubeSats. On the other hand, single-stage architectures are actively investigated for smaller satellites [100] and exploration rovers [101].

2) *Multi-stage Architecture*: This architecture is popular in CubeSat applications wherein multiple power conversion stages such as single-input-single-output (SISO) converters are used with dedicated functionality [27]–[31], [36]–[95]. For example, PV-side converters are designed to perform MPPT tracking and load-side converters are designed for regulating output voltages. Both the architectures shown in Fig. 4 (a)-(b) are a type of multi-stage. As each converter can be optimally designed to meet their respective functionality, it has lower control complexity and better system performance under wide range of operating conditions. However, it has trade-off with total component count and lower system efficiency due to multiple conversion stages. It should be noted that the several COTS EPS designs of CubeSats utilize multi-stage architecture [27]–[31].

#### IV. OPERATION PRINCIPLES OF EPS ARCHITECTURES

This section presents the operational details of different EPS architectures with focus on the type of PV panel interface and dc-bus voltage regulation.

##### A. Architectures with DET and Unregulated Dc-bus

The EPS architectures with DET and unregulated dc-bus voltage are shown in Fig. 6. In case of EPS-1 shown in Fig. 6 (a), the output of PV panels is connected to battery in parallel with shunt regulator and the load-side converters for further conversion [36]–[41]. The PV panel's output voltage is clamped to floating battery voltage and its output current depends on the I-V characteristics curve. The battery feeds to loads directly during the eclipse period and it has protection system to avoid over-current, over-voltage, and under-voltage conditions. It has higher conversion efficiency due to power conversion by just one dc-dc converter before feeding the load demand.

In [36], EPS-1 architecture is developed for OUFT1-1 1U CubeSat with dc-bus voltage varying between 2.7 to 4.2 V. It has 3.3 V, 5 V, and 7.2 V regulated voltages for the loads and it uses two Li-ion batteries in parallel for redundancy. In [37], EPS-1 is implemented for CPI 1U CubeSat with nominal dc-bus voltage of 3.6 V. The solar panels have two cells connected in series with nominal voltage of 4.2 V. It uses Lithium metal as primary battery and three Li-ion cells in parallel as secondary battery. The load-side converters provide regulated voltages 3.6 V and 5 V. For PilsenCube II 1U CubeSat [38], EPS-1 is developed with three independent supply channels for redundancy. In two of the supply channels, EPS-1 is used with unregulated dc-bus voltage varying between 3 V to 4.2 V. On the generation-side, each solar panel uses 24 triple junction solar cells in series/parallel combination. In [40], EPS-1 with super-capacitor as the energy storage is tested in order to improve the reliability of EPS. In this case, the dc-bus voltage varies up to 2.7 V and two regulated voltages of 3.3 V and 5 V are provided for the loads. For Kysat-3 1U CubeSat, distributed EPS-1 with solar module, battery module, and

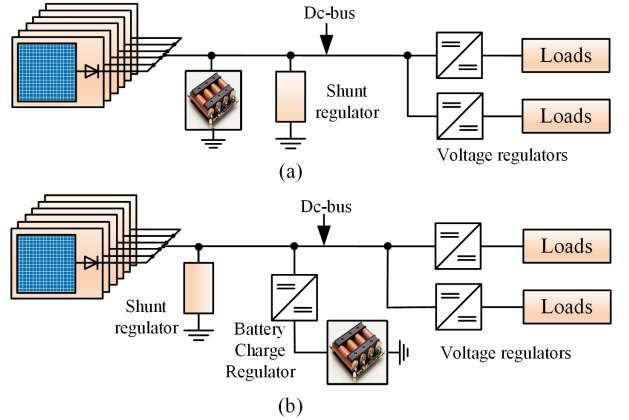


Fig. 6. Architectures with DET and unregulated dc-bus. (a) EPS-1 (b) EPS-2.

payload modules are implemented with synchronous rectifiers as the DET interface to reduce the conduction losses [41].

The EPS-2 architecture is shown in Fig. 6 (b) [43]–[45]. It has the output of the PV panels connected directly to shunt regulator and load-side converters and the battery is interfaced to the dc-bus via the battery charge regulator (BCR). The BCR is responsible for regulating the battery voltage and charging current using two control loops. There will be power losses in one dc-dc converter when the PV panels supply load demand, whereas the power losses occur in two converters when the battery supplies load demand. Thus, it has lower efficiency compared to EPS-1, and also, lower reliability due to additional points of failure introduced by the BCR.

In [43], EPS-2 architecture is implemented with dedicated BQ2405 charger connected to two series connected 1000 mAh Li-ion batteries. For the QuakeSat 3U CubeSat [44], EPS-2 is developed with two sets of BCRs connected to two Li-ion cells in series. The power source consists of twelve solar arrays, four of which are body mounted and rest of them are deployable. On the load-side, regulated voltages of +5V and -5V are supplied to the payloads and some of the equipment are connected to unregulated dc-bus. Also, EPS-2 is used in Inusat-1 CubeSat with dc-bus voltage varying between 12 to 30 V [45]. It uses two series connected lithium polymer batteries with voltage rating 12 to 16.8 V and provides regulated voltages 5 V, 12 V, and 13.6 V to the loads.

##### B. Architecture with DET and Regulated Dc-bus

The EPS architectures with DET and regulated dc-bus voltage are shown in Fig. 7. The EPS-3 illustrated in Fig. 7 (a) utilizes voltage regulator connected in series with the load-side converters to provide regulated dc-bus to the load equipment [89]. In EPS-3, the conversion losses occur in the two converters when the PV panel or battery supplies the load demand. In comparison to EPS-1, it has lower efficiency, higher component count, and less reliability due to additional points of failure introduced by the voltage regulator.

The EPS-4 architecture illustrated in Fig. 7 (b) is similar to the EPS-2 except that the function of dc-dc converter interfacing the battery is different [89]. The voltage regulator of battery maintains the dc-bus voltage close to reference value during the sunlit period and eclipse period by balancing the

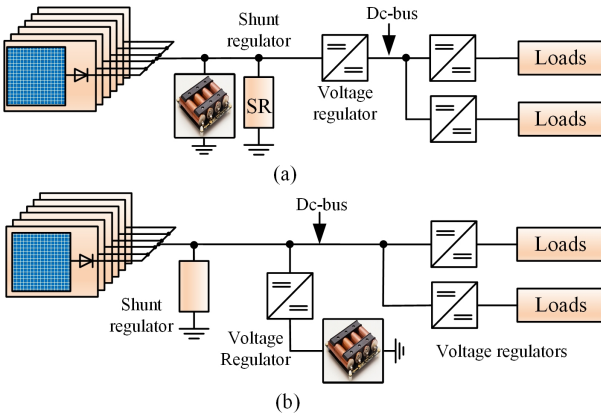


Fig. 7. Architectures with DET and regulated dc-bus. (a) EPS-3 (b) EPS-4.

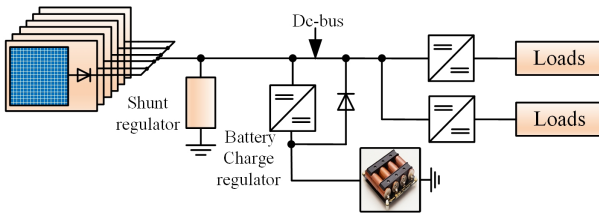


Fig. 8. EPS-5: Architecture with DET and sun-regulated dc-bus.

power difference between generation and load demand. In case the battery is fully charged, shunt regulator is used to maintain the dc-bus voltage by absorbing the excess power. Both EPS-3 and EPS-4 are not used in any CubeSat EPS designs as of now.

#### C. Architecture with DET and Sun-regulated Dc-bus

The EPS-5 architecture is almost similar to EPS-2 except for the battery discharge diode between dc-bus and the battery as illustrated in Fig. 8, which is commonly used in bigger satellites [7]. In EPS-5, the shunt regulator is used in the sunlit period to regulate the dc-bus voltage and the BCR is used to regulate the charge current of the battery in a constant current-constant voltage mode. During eclipse period, the BCR is disabled and the battery discharges directly to loads via diode avoiding the conversion losses. Thus, the dc-bus voltage is regulated during the sunlit period only. Assuming that low-loss diode is used, it has lower conversion losses compared to EPS-2 and EPS-3 but higher than EPS-1. This architecture is not used in any CubeSat EPS designs until now.

#### D. Architectures with PPT and Unregulated Dc-bus

The EPS architectures with series connected MPPT converter and unregulated dc-bus are shown in Fig. 9. In the EPS-6 shown in Fig. 9 (a), a MPPT converter is connected in series with one set of PV panels and their output is directly connected to battery terminals [27]–[31], [46]–[68], [70], [71]. If the voltage of battery exceed upper limit, the MPPT converter operates in the voltage regulation mode to maintain the battery voltage at the maximum value. In this case, the PV panels supply power equal to the load demand and conversion losses. The load demand is processed by two converters when the

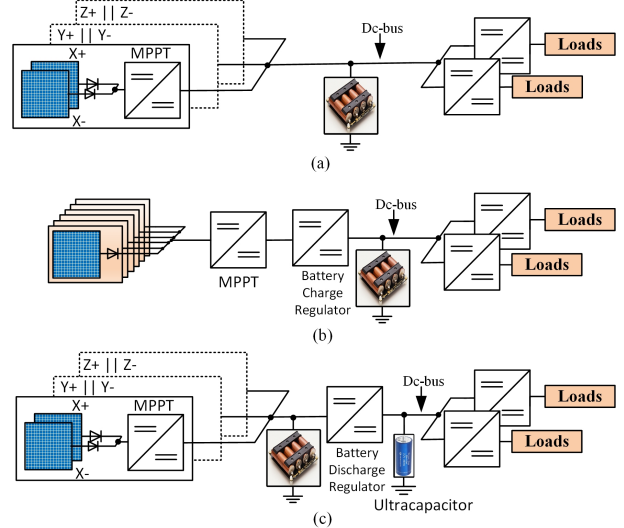


Fig. 9. Architectures with PPT and unregulated dc-bus. (a) EPS-6, (b) EPS-7, and (c) EPS-8.

PV panels supply it, whereas the battery supply to load is processed by one dc-dc converter.

The EPS-6 architecture is commonly used in several COTS EPS designs such as GOMspace [27], [28], Crystalspace [29], Clydespace [30], and Nanoavionics [31]. The GOMspace has implemented this for 1U-3U CubeSats with PV power up to 30 W [27], and modular EPS architecture is developed for CubeSats larger than 3U with PV power up to 300 W [28]. The Crystalspace has developed it for 1U-2U CubeSats with ratings up to 10 W continuous solar input and 3.3 V, 5 V, 12 V, unregulated 3.7 V supply. It has two MPPT converters with each converter having input from the three parallel connected PV panels. The AAC Clydespace has products based on EPS-6 for 1U CubeSat with integrated battery, 2U and 3U CubeSats with body mounted panels, 3-12U CubeSats with deployable panels [30]. The Nanoavionics has developed EPS-6 with wide range solar input from 2.6-18 V and 3.3 V, 5 V, 3-18 V configurable voltages [31].

In [47], the design and implementation of EPS-6 for 2U CubeSat using a single-ended primary-inductor converter (SEPIC) is presented. The main reason for selecting SEPIC converter is due to advantages of input current continuity, voltage boosting and bucking, short circuit protection, low-side driver, and non-inverted input and output voltages. In PiCPoT CubeSat, EPS-6 is used with MPPT converter made with hysteretic switching converter and six battery packs divided into two groups [48]. This architecture is also used in a 12U CubeSat named Aoxiang-Sat with solar panels having output power of 57.7 W and six battery cells (2S3P) with 57.72 Wh rating [51], [52].

For a 3U CubeSat, EPS-6 is deployed with the MPPT algorithm executed in both analogue and digital controllers to achieve redundancy [53]. In ERPSat-1 1U CubeSat, EPS-6 is implemented with a fuzzy logic algorithm for MPPT, better power management, and efficient energy distribution among subsystems [57]. For a 3U CubeSat named Libertad 2 [58], this architecture is deployed after evaluating the different operating conditions in terms of efficiency of power converters. In the Ncube 1U CubeSat, EPS-6 is implemented with only

one MPPT converter by connecting all the PV panels in parallel and on the load-side POL converters are used to feed the different loads [70]. The ESTCube-1 CubeSat which has performed first in-orbit electric solar wind sail experiment also utilized EPS-6 with redundant components to ensure that component failures would not jeopardize the mission [59]. The in-flight results showed that component failures did not cause any major problems and system efficiency is improved due to parallel operating converters. On the other hand, this CubeSat design had challenges due to several components duplicated in hot redundant configuration, which lead to high software complexity to control and monitor the redundant systems.

In [66], EPS-6 is developed with a buck type SCC for MPPT in an 8 Kg remote sensing nano-satellite. It achieved higher power density due to absence of inductors and a novel method of MPPT is presented which involves the measurement of the PV panel voltage, PV panel temperature, and computing the sun incidence angle with the knowledge of the space craft position. This architecture is also implemented in SPICA and Puerto Rico CubeSats with SEPIC for MPPT tracking and 3.3 V and 5 V regulated output voltages [49], [68]. In [54], details of EPS-6 used in MYSAT-1 are presented along with operational modes.

In the EPS-7 architecture shown in Fig. 9 (b) [72], [73], all the PV panels are connected in parallel and then connected to a dc-dc converter for MPPT operation. The MPPT converter is cascaded by a BCR to regulate the charging current of battery in order to ensure long-life of Li-ion batteries. The main disadvantage of EPS-7 is lower efficiency as solar power needs to be processed by three converters before feeding to the loads. In Swayam 1U CubeSat [72], [73], EPS-7 is implemented with boost converter for MPPT operation which steps up the unregulated PV panel voltage to 5 V and battery consists of two parallel connected NCR18650A Li-ion cells with nominal voltage of 3.6 V. The EPS uses TPS64200 integrated circuit (IC) to provide regulated bus voltage of 3.3 V for the load equipment and Texas Instrument's Bq24002 is used for battery charge regulation.

The EPS-8 architecture displayed in Fig. 9(c) is used in CubeSats with hybrid energy storage, wherein UC is required due to the peaky loads [74]. The output of MPPT converters is connected to battery terminals and the UC is connected to the load-side dc-dc converters. A battery discharge regulator (BDR) is placed in between battery and UC to limit the current drawn from the batteries to rated value. In EPS-8, the load power gets processed thrice or twice or once when it is supplied by PV panels, batteries, and UC, respectively. This EPS-8 is commercially available with operating temperature range of -40 to 50 °C and it is recommended for CubeSats with peaky loads such as SAR and LIDAR.

The hybrid EPS architectures which combines direct energy transfer with peak power tracking capability are illustrated in Fig. 10 [75]–[87]. The EPS-9 architecture was originally proposed for Generic Nanosatellite Bus developed by University of Toronto [76]. It is similar to EPS-2 (excluding shunt regulator) except that the parallel connected dc-dc converter operates as MPPT converter in two-loop control mode to regulate both the dc-bus voltage as well as to limit the charging

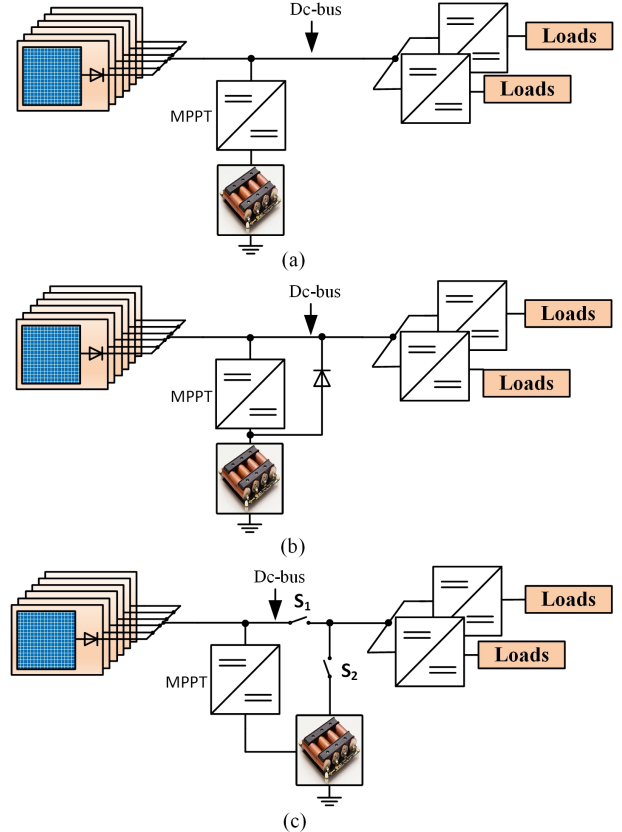


Fig. 10. Architectures with PPT and unregulated dc-bus. (a) EPS-9, (b) EPS-10, and (c) EPS-11.

current. During sunlit period, the dc-bus voltage is regulated at MPP voltage and when the battery is fully charged, the dc-bus voltage will be regulated at maximum battery voltage. In EPS-9, the load power gets processed once when supplied by PV panels, whereas it gets processed twice when supplied by batteries. Compared to EPS-6, this architecture has the lowest conversion losses when the PV panels meet most of the load demand, but some failures in MPPT converter may isolate the battery storage leading to partial or full loss of CubeSat mission. It is implemented in MEROPE 1U CubeSat with MAX1757 IC as a MPPT converter, and two polystyrene prismatic Li-ion cells in parallel with a nominal voltage of 3.7 V [75]. Also, this architecture is implemented in one of the EPS of Tel-USat by using SPV1040 IC for MPPT, Li-ion battery having nominal voltage of 7.4 V, and with 3.3 V, 5 V regulated output voltages [77].

In the EPS-10 architecture shown in Fig. 10(b), the battery is interfaced to dc-bus via the diode in addition to the MPPT converter. The MPPT converter operates only in sunlit period to maintain the dc-bus voltage close to MPP voltage [78]–[84]. The battery gets charged or discharged depending on whether load demand is lower or higher than the power generation, respectively. When the battery is fully charged, the MPPT converter regulates the dc-bus voltage such that PV panels supply only load demand and conversion losses. During eclipse period, the MPPT converter will be disabled so that dc-bus voltage falls down and the diode gets forward biased facilitating the battery to directly supply the loads. Compared to EPS-9, the conversion losses are reduced during battery

discharge mode in eclipse period. One disadvantage of EPS-10 is the constraint on the battery design as the maximum battery voltage should be lower than MPP voltage at full irradiation to avoid forward biasing of diode during sunlit period. This architecture is used in Ibeos' 150 W EPS with regulated 3.3 V, 5 V, and 12 V power through current-limited outputs [78]. It is also implemented in 3U CubeSat developed by Santa Clara University [79], which used two series connected Li-ion cells with nominal voltage of 7.4 V. This EPS has regulated 5 V and 12 V power output and the transmission beacon is directly connected across the UC. In TTUSat 1U CubeSat [80], EPS-10 is implemented with LT3652IC as a MPPT converter and two Li-ion cells in parallel. In this CubeSat, a boost converter is used in series with MPPT converter due to lower input voltage from the PV panels. Also, two sets of MPPT converter and battery cells are used in order to improve the reliability of EPS. In Cute-1.7+APD II nano-satellite [81], [82], EPS-10 is developed with four Li-ion cells and has provision of 3.3 V, 5 V, 6 V and 7 V stabilized buses. In IITMSAT [83], this architecture is implemented with LT3652 IC as battery charger, two series connected Li-ion cells, and 3.3 V and 5 V regulated voltage buses. Also, the AHAN CubeSat has used EPS-10 with the modification that every PV panel had separate MPPT converter and their output is connected in parallel to the battery [84]. This gives the advantage of higher reliability in case of failure of MPPT converter.

In Fig. 10(c), EPS-11 architecture with reconfigurable switches is illustrated [85]–[88]. During sunlit period, the switch  $S_1$  is turned on and  $S_2$  is turned-off and then, the circuit configuration and operation become similar to EPS-9. During eclipse period, the switch  $S_1$  is turned off and  $S_2$  is turned-on so that battery supplies the loads directly. During eclipse period, the circuit operation is similar to EPS-10 except that transistor switch is used instead of diode. EPS-11 is experimentally validated by using gallium nitride (GaN) field-effect transistors (FET) with device switching frequency of 500 KHz. It is demonstrated to be modular and scalable for any number of subsystem voltages, payload requirements, and size of CubeSat [85]. In addition, the path selection switches can be selected to improve the conversion efficiency based on the power generation and load demand during the sunlit period. For example, the switches  $S_1$  should be turned-on and  $S_2$  should be turned-off if the solar panels can meet most of the power demand, whereas, the switches  $S_1$  should be turned-off and  $S_2$  should be turned-on if the battery meets most of the power demand. In case of failure in MPPT converter, the switches  $S_1$  and  $S_2$  can be operated to ensure the continuity of power supply to load-equipment.

#### E. Architectures with PPT and Regulated Dc-bus

The regulated dc-bus PPT architectures are shown in Fig. 11 and Fig. 12, wherein the dc-bus voltage is regulated close to the reference value by using an additional dc-dc converter. In the EPS-12 architecture shown in Fig. 11 (a), the MPPT converter is placed in series with the PV panels and it's output is directly connected to battery terminals [38]. The voltage regulator for dc-bus appears in series with loads. The power

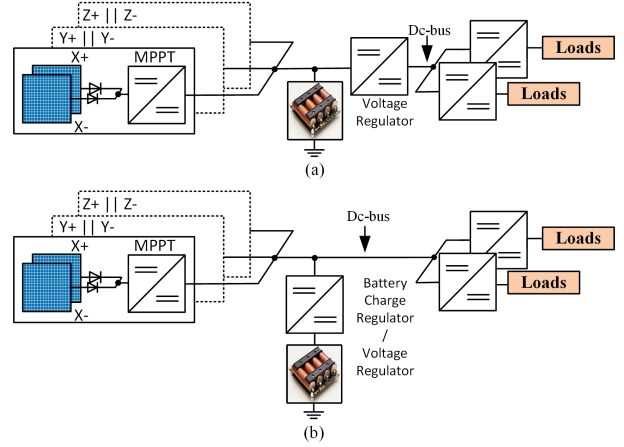


Fig. 11. Architectures with PPT and regulated dc-bus. (a) EPS-12, and (b) EPS-13.

needs to be processed by three power converters when the PV panels supply loads, whereas the power gets processed by two converters when the battery supplies load demand. In PilsenCube II 1U CubeSat, EPS-12 is implemented in one of the power supply channels with UC as energy storage and the dc-bus voltage is regulated at different voltages in the range of 3.4 V to 4.9 V [38].

The EPS-13 architecture is illustrated in Fig. 11(b), wherein there is flexibility in battery selection as the battery voltage can be anywhere within the converter duty cycle limits and also, it provides possibility of using higher dc-bus voltage with lower currents leading to lower conduction losses [7]. This architecture has two different ways of operation. In the first case, MPPT converter has additional function of keeping dc-bus voltage at a given reference value and the BCR regulates the charging and discharging currents of battery [90]. It is implemented in 2U CubeSat named Parikshit with SPV1040 IC as MPPT converter, LTC4066 IC as a battery charger, three Li-ion batteries in parallel with nominal voltage of 3.7 V, and loads are supplied with regulated voltages equal to 3.3 V, 4.2 V, and 5 V [90].

In the second case, the parallel connected dc-dc converter acts as voltage regulator to maintain the dc-bus voltage at given reference value [91]–[93]. In this, the battery operates in discharging mode during the eclipse period via dc-dc converter and during sunlit period, battery gets charged or discharged via dc-dc converter depending on the load demand. When the voltage of battery hits upper limit, the MPPT converter regulates the dc-bus voltage to the maximum battery voltage, which means that PV panels just supply load demand and losses in converter. In EPS-13, the power need to be processed by two power converters whether the PV panels or batteries supply load demand. This architecture is implemented in RVSAT-1 2U CubeSat with two series and two parallel Li-ion batteries and it provides 3.3 V, 5 V, and unregulated bus to the load equipment [92]. In [93], EPS-13 is studied with focus on the energy generation, storage, and their sizing guidelines.

In the EPS-14 architecture shown in Fig. 12 (a) [77], all the PV panels are connected in parallel and their output is connected to a voltage regulator. The output of the regulator is connected to the load-side converters as well as the battery charger with MPPT functionality. The power is processed by

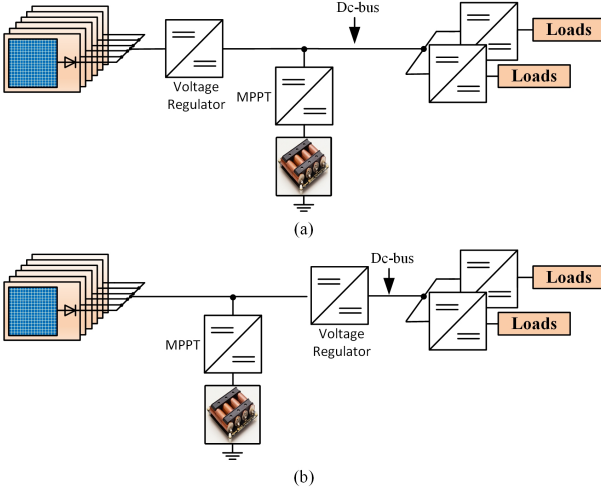


Fig. 12. Architectures with PPT and regulated dc-bus. (a) EPS-14, and (b) EPS-15.

two converters whether PV panels or battery supply load demand. It is implemented in Tel-USat EPS with 12 V regulated dc bus. It used LM2577-12 IC as voltage regulator, LT3652 IC for MPPT, Li-ion battery having nominal voltage of 7.4 V, and the loads were supplied with 3.3 V, and 5 V regulated output voltages [77].

In the EPS-15 architecture displayed in Fig. 12(b), all the PV panels are connected in parallel and their output is fed to the MPPT converter as well as the voltage regulator for dc-bus [94]. The MPPT converter regulates the PV panels output voltage to MPP voltage and the dc-bus voltage is regulated by another dc-dc converter. In EPS-15, the power gets processed by two power converters when the PV panels supply the load demand, whereas three power converters process the power when the batteries supply load demand [70]. In EPS-15 and EPS-16, the open-circuit failure of semiconductor device lead to disconnection of loads from PV and/or battery and thus, leading to loss of CubeSat mission.

#### F. Architectures with PPT and Sun-regulated Dc-bus

The sun-regulated dc-bus PPT architectures are shown in Fig. 13 [89], [95]. In the EPS-16 architecture shown in Fig. 13 (a), the voltage regulator maintains the dc-bus voltage close to the reference value and the battery gets charged or discharged depending on whether the load demand is lower or higher than power generation, respectively. When the battery is fully charged, the MPPT converter maintains the dc-bus voltage at maximum battery voltage so that PV panels supply the load demand and conversion losses. During eclipse period, the voltage regulator is disabled and the diode is automatically forward biased leading to battery supplying power to the loads. In [95], EPS-16 is implemented with two series connected Li-ion cells and distributed POL converters to achieve higher efficiency.

An additive stacking configuration based sun-regulated dc-bus architecture is illustrated in Fig. 12 (b) [89]. In this EPS-17, both the voltage regulator and MPPT converters are placed in parallel across the PV panel. The output of the voltage regulator and MPPT converters are connected in series to create the dc-bus voltage. The voltage regulator maintains the

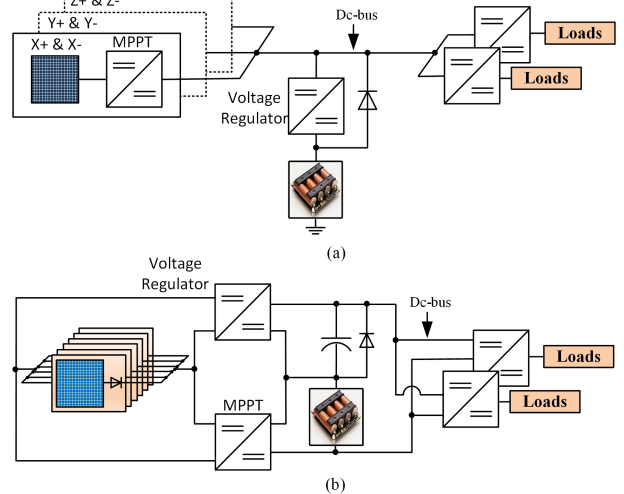


Fig. 13. Sun-regulated dc-bus PPT Architectures. (a) EPS-16, and (b) EPS-17.

dc-bus voltage to a reference value and it should be a voltage boost converter as the dc-bus voltage is always higher than the PV panel voltage. The MPPT converter should be a buck-boost converter to allow different combinations of PV panel and battery ratings. The MPPT algorithm provides the reference current for the battery charge control. The main advantage of EPS-17 is reduced conduction losses due to higher dc-bus voltage. During the eclipse period, the voltage regulator is disabled so that the diode gets forward biased and the battery directly supplies to the loads.

#### V. COMPARISON OF EPS ARCHITECTURES

The summary of the seventeen EPS architectures is given in Table. IV. The column “Flight heritage” indicates whether the EPS architecture is utilized in actual CubeSat mission or not. It can be noticed that ten out of the seventeen architectures are used real CubeSat missions and among them, three EPS architectures (EPS-6, EPS-8, and EPS-10) are commercially available. Other architectures such as EPS-3 to EPS-5 and EPS-15 to EPS-17 are in the research and development stage and to best of our knowledge, they have been not utilized in any CubeSat mission until now. The general trend in CubeSat missions is to use COTS products but some developers have been preferring to develop their own EPS architectures. Also, most of the architectures are centralized type due to volume and weight constraints of CubeSats and all the existing EPS architectures use multiple conversion stages due to simplicity and rich flight heritage. Out of the ten EPS architectures with flight heritage, seven architectures use unregulated dc-bus architecture to achieve higher efficiency and lower component count. Due to the limited power generation capacity, most of the EPS architectures with flight heritage, except EPS-1 and EPS-2, are using MPPT for the PV panels.

A comparison of discussed seventeen EPS architectures in terms of power conversion stages used, and number of components required is given in Table V. It includes the number of power converters between PV panel to load, battery to load, PV panel to battery, total number of power converters, number of passive components, and the total number of semiconductor

TABLE IV  
SUMMARY OF THE CUBESAT EPS ARCHITECTURES

Architecture	Flight heritage	Commercial Products	Converters location	Interface of PV panels	Dc-bus regulation	References	Mission Names
EPS-1	Yes	No	Centralized	DET	Unregulated	[36]–[40]	OUFTI-1, CP1, PilsenCube II
	Yes	No	Distributed	DET	Unregulated	[41], [42]	KySat-2
EPS-2	Yes	No	Centralized	DET	Unregulated	[43]–[45]	GOLIAT, QuakeSat
EPS-3	No	No	Centralized	DET	Regulated	[89]	Not used
EPS-4	No	No	Centralized	DET	Regulated	[89]	Not used
EPS-5	No	No	Centralized	DET	Sun-regulated	[7]	Not used
EPS-6	Yes	Yes	Centralized	PPT	Unregulated	[27]–[31], [46]–[69]	Floripasat-1,NutSat,MYSAT-1
	Yes	No	Distributed	PPT	Unregulated	[70], [71]	Ncube
EPS-7	Yes	No	Centralized	PPT	Unregulated	[72], [73]	Swayam
EPS-8	Yes	Yes	Centralized	PPT	Unregulated	[74]	No information
EPS-9	Yes	No	Centralized	PPT	Unregulated	[75]–[77]	MEROPE, Tel-USat, CanX-4&5
EPS-10	Yes	Yes	Centralized	PPT	Unregulated	[78]–[84]	Cute-1.7, IITMSAT
EPS-11	No	No	Centralized	PPT	Unregulated	[85]–[88]	Not used
EPS-12	Yes	No	Centralized	PPT	Regulated	[38]	PilsenCube II
EPS-13	Yes	No	Centralized	PPT	Regulated	[90]–[93]	RVSAT-1
EPS-14	Yes	No	Centralized	PPT	Regulated	[77]	Tel-USat
EPS-15	No	No	Centralized	PPT	Regulated	[94]	Not used
EPS-16	No	No	Distributed	PPT	Sun-regulated	[95]	Not used
EPS-17	No	No	Distributed	PPT	Sun-regulated	[89]	Not used

devices in the power circuit. The efficiency of EPS architecture depends on the number of power conversion stages which changes depending on the load profile and power generation. During eclipse period, the battery is the only source to provide the power supply to the loads and thus, the number of power converters between battery to loads determines the power conversion losses. During sunlit period, the total number of power conversion stages depends on whether the load demand is higher or lower than the power generation. If the load demand is less than the power generation, the number of power converters between PV to load and PV to battery determine the power conversion losses. If the load demand is higher than power generation, the number of power converters between PV to load and battery to load determines the overall conversion losses. It should be noted that some of the architectures such as EPS-5, EPS-10, and EPS-16 have bypass diode across the power converter. This bypass diode gets forward biased during the eclipse period and thus, the number of power conversion stages between battery to load should be reduced by one. Also, the EPS-11 architecture utilizes reconfigurable switches and thus, the number of power conversion stages between PV to load and battery to load changes depending on whether  $S_1$  or  $S_2$  is turned on. Table V shows the number of conversion stages in EPS-11 when  $S_1$  is turned-on. To evaluate the efficiency of architecture, it is recommended to take the complete mission parameters and load profile for all the modes of operation [35].

For the CubeSats, the total number of components in the EPS architecture are crucial due to strict volume and weight constraints. The last column of the Table V shows the total number of components in the main power circuit. The shunt

regulator is considered to have one switch and one resistor, and each PV panel is connected in series with a blocking diode. The DET architectures (EPS-1 to EPS-5) have the lowest number of components, but it has trade-off with the power extraction from the PV panels. To compare the PPT architectures, they need to be further classified based on configuration of PV panels:

- 1) All PV panels connected in parallel (EPS-7, EPS-9, EPS-10, EPS-11, EPS-14, EPS-15, and EPS-17).
- 2) PV panels on opposite sides of CubeSat are connected in parallel to a MPPT converter (EPS-6, EPS-8, EPS-12, EPS-13, and EPS-16).

In the above classification, the first type of architectures has the lowest number of components compared to second type due to lower number of MPPT converters. However, these architectures have possibility of losing entire power generation if there is a short-circuit failure of switch in the dc-dc converter connected in parallel across the PV panels. In this fault case, the PV panels get connected to the battery that decides the operating point of PV panels. If the battery voltage is higher than the open-circuit voltage of PV panel, the PV panels cannot supply power to the battery and loads. To summarize, it is important to evaluate all the aspects, for example, efficiency, number of components, and reliability, while selecting the best possible EPS architecture for a given CubeSat mission. Table V thus can provide an overview on the different components involved and can help to foresee the EPS's relative size.

## VI. FUTURE SCOPE OF RESEARCH

One of the important research area to be focused is on improving the reliability of CubeSat EPS. The CubeSat database

TABLE V  
COMPARISON OF CUBESAT EPS ARCHITECTURES

Architecture	Number of Converters Between PV to Load	Number of Converters Between Battery to Load	Number of Converters Between PV to Battery	Total Number of Converters	Number of Passive Components	Number of Semiconductor Devices	Total Number of Components
EPS-1	1	1	0	2	7	11	18
EPS-2	1	2	1	4	10	13	23
EPS-3	2	2	0	4	10	13	23
EPS-4	1	2	1	4	10	13	23
EPS-5	1	2	1	4	10	14	24
EPS-6	2	1	1	4	15	16	31
EPS-7	3	1	2	6	12	14	26
EPS-8	3	2	1	6	18	18	36
EPS-9	1	2	1	4	9	12	21
EPS-10	1	2	1	4	9	13	22
EPS-11	1	2	1	4	9	14	23
EPS-12	3	2	1	6	18	18	36
EPS-13	2	2	2	6	18	18	36
EPS-14	2	2	2	6	12	14	26
EPS-15	2	3	1	6	12	14	26
EPS-16	2	2	2	6	18	19	37
EPS-17	2	1	1	4	13	15	28

shows that EPS failure has been one of the major factor in breakdown of CubeSats [102]. The main reason is due to weight limit of CubeSat which prevents usage of heavy shielding materials to protect the CubeSat from the ionizing radiation in the cosmic environment [38], [103]. To improve the reliability of EPS, redundancy for critical components has to be ensured in the event of single-event upset. However, the space constraints on the PCB of EPS limit the placement of the redundant components [104]. This issue can be solved either by reducing the size of passive components and/or by minimizing the number of passive components especially the inductors with bigger footprints.

One solution to reduce the footprints of passive components is by operating the converters at high switching frequency by utilizing wide band-gap semiconductor devices such as GaN FET [86], [87]. These devices provide higher performance, lower device losses, smaller footprints, and robust in harsh radiation environment [105]. Another solution is to innovate and develop novel multiport converter topologies for CubeSats EPS which offer several advantages such as smaller footprints, higher conversion efficiency, cheaper solution, etc. This research topic has lot of potential for further exploration and innovation as there are no publications or patents focusing on multiport converters for the CubeSats EPS until now. Also, the research should focus on developing new system architectures that achieve smaller footprints by minimizing the energy storage requirements of passive components without compromising on the performance. It should be highlighted that, all the EPS architectures with flight heritage are using multi-stage configuration with several SISO converters as illustrated in Fig. 2.

In the literature, several multiport converters have been proposed for various applications, such as, DC microgrid, PV-battery systems, electric vehicles, hybrid energy storage system, and bigger satellites [106]–[122]. Among them, one of the most suitable converter for CubeSat application is the

three-port dc-dc converter (TPC) [123]. The TPC can be further divided into three categories: isolated [109], partially isolated [110]–[114], and non-isolated [115]–[122]. The non-isolated TPCs could be more attractive over isolated and partially isolated TPCs due to their smaller footprints. The researchers should focus on evaluating these suitable topologies with respect to COTS CubeSat EPS in terms of control complexity, footprint and overall efficiency. Also, the multiport converter topologies with single inductors or switched capacitor converters (SCC) will have smaller footprints and thus, suitable for CubeSats which have strict volume and weight constraints [124]. The research challenge in developing multiport converters for CubeSats may arise due to wide varying irradiation conditions on the PV panels in the LEO missions (excluding some deployable panel based CubeSats), which is uncommon in terrestrial PV systems. It should be highlighted that the problem of irradiation mismatch conditions in terrestrial PV applications has been solved by using distributed MPPT solutions [125]. However, the existing solutions need to be thoroughly investigated for CubeSats EPS as there exists 100% mismatch in irradiation conditions as well as volume and weight constraints. All these system constraints and performance requirements provide new research opportunities for further exploration and innovation.

The possible multi-stage CubeSat EPS architectures using multiport converter topologies such as multiple-input-single-output (MISO), and single-input-multiple-output (SIMO) converters are shown in Fig. 14. The configuration 1 utilizes MISO converters for the PV panels and SIMO converter for the load-side equipment, configuration 2 uses MISO converters for the PV panels and multiple SISO converters for load-side equipment, and configuration 3 uses multiple SISO converters for the PV panels and SIMO converter for the load-side equipment. The state-of-the-art EPS with multiple SISO converters requires largest footprint but it has lowest control complexity as each converter needs to handle only part of the system

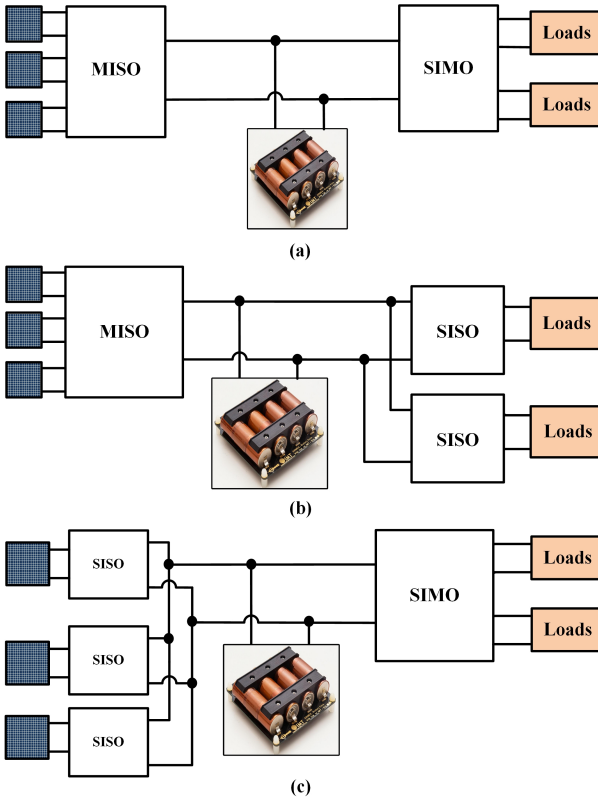


Fig. 14. Possible multi-stage CubeSat EPS architectures: (a) Configuration 1, (b) Configuration 2, and (c) Configuration 3.

requirements. Let us consider that each multiport converter utilizes a maximum of one inductor, which dominates all other components in terms of footprint. The configuration 1 is advantageous in terms of smaller footprint area but it has higher control complexity due to coupling between different system variables. The configurations 2 and 3 have slightly higher control complexity but has smaller footprint compared to the state-of-the-art EPS. All these configurations can be considered like midway solution between single-stage EPS (MIMO based) and the state-of-the-art EPS.

Another research area to be focused is developing sophisticated EPS architectures which achieves smaller footprints by reducing the energy storage requirements of passive components especially inductors. The emerging power conversion architectures such as merged multi-stage power conversion need to be investigated for CubeSats EPS. This architecture is an intermediate solution between single-stage and multi-stage architectures, wherein multiple conversion stages are merged functionally or topologically [99]. It has reduced number of components, achieve higher efficiency due to lesser conversion stages, better device utilization, and enhanced reliability compared to multi-stage architectures.

## VII. CONCLUSION

A comprehensive review of CubeSat EPS architectures is presented in this paper. The EPS is the critical subsystem in the CubeSats as it powers all other subsystems. The first step in EPS design is the selection of EPS architecture which should be done based on overall efficiency, simplicity of control, component count, flexibility in battery configuration, reliability,

and fault-tolerant capability. The existing EPS architectures are classified based on the number of power conversion stages, location of power converters, interfacing of PV panels, and type of dc-bus voltage regulation. All the existing EPS architectures are classified into seventeen categories and their operation details are presented along with their advantages and disadvantages. It is expected that this paper becomes a useful reference guide for CubeSat developers who are working on custom EPS designs and for the researchers who are working towards developing next generation EPS architectures.

## REFERENCES

- [1] H. Heidt, J. Puig-Suari, A. Moore, S. Nakasuka, and R. Twiggs, "Cubesat: A new generation of picosatellite for education and industry low-cost space experimentation," in *Proc. 14th Annu AIAA/USU Conf. Small Satellites*, vol. 91, 2000, pp. 894–900.
- [2] I. Nason, J. Puig-Suari, and R. Twiggs, "Development of a family of picosatellite deployers based on the cubesat standard," in *Proc. IEEE Aerosp. Conf.*, vol. 1, March 2002, pp. 1–1.
- [3] M. N. Sweeting, "Modern small satellites-changing the economics of space," *Proc. IEEE*, vol. 106, no. 3, pp. 343–361, March 2018.
- [4] K. O. et al., "Tokyo Tech 1kg Pico-Satellite CUTE-I-Development, Launch & Operations," in *Proc. IFAC Symp. Auto. Contr. Aero.*, vol. 37, no. 6, June 2004, pp. 931–936.
- [5] M. Swartwout, "Cubesat-database." [Online]. Available: <https://sites.google.com/a/slu.edu/swartwout/home/cubesat-database>
- [6] ———, "Nanosats database." [Online]. Available: <https://www.nanosats.eu/database>
- [7] M. R. Patel, *Spacecraft Power Systems*, 1st ed. Boca Raton, Florida, USA: CRC PRESS, November 2004.
- [8] K. Woellert, P. Ehrenfreund, A. J. Ricco, and H. Hertzfeld, "Cubesats: Cost-effective science and technology platforms for emerging and developing nations," *Adv. Space Res.*, vol. 47, no. 4, pp. 663–684, 2011.
- [9] A. Klesh and J. Krajewski, "Marco: Cubesats to mars in 2016," in *Proc. 29th Annu AIAA/USU Conf. on Small Satellites*, August 2015.
- [10] B. K. Malphrus, K. Z. Brown, J. Garcia, C. Conner, J. Kruth, M. S. Combs, N. Fite, S. McNeil, S. Wilczewski, K. Haught, A. Zucherman, P. Clark, K. Angkasa, N. Richard, T. Hurford, D. Folta, C. Brambora, R. MacDowall, P. Mason, S. Hur-Diaz, J. Breeden, R. Nakamura, A. Martinez, and M. M. Tsay, "The lunar icecube em-1 mission: Prospecting the moon for water ice," *IEEE Aerosp. Electron. Syst. Mag.*, vol. 34, no. 4, pp. 6–14, 2019.
- [11] R. Pothamsetti and J. Thangavelautham, "Photovoltaic electrolysis propulsion system for interplanetary cubesats," in *Proc. IEEE Aero. Conf.*, 2016, pp. 1–10.
- [12] M. A. Johnson, P. Beauchamp, H. Schone, C. Venturini, L. Jasper, R. Robertson, M. Moe, J. Leitner, and F. Tan, "The small satellite reliability initiative: A public-private effort addressing smallsat mission confidence," in *Proc. 32th Annu AIAA/USU Conf. Small Satellites*, August 2018.
- [13] L. Jacques, "Thermal Design of the Oufti-1 nanosatellite," Master's thesis, University of Liège, Liège, Belgium, 2009.
- [14] P. Reiss, P. Hager, C. Bewick, and M. MacDonald, "New methodologies for the thermal modeling of cubesats," in *Proc. 26th Annu AIAA/USU Conf. Small Satellites*, June 2012, pp. 1–12.
- [15] J. J. Soon, J. W. Chia, H. Aung, J. M. Lew, S. T. Goh, and K. Low, "A photovoltaic model based method to monitor solar array degradation on-board a microsatellite," *IEEE Trans. Aerosp. Electron. Syst.*, vol. 54, no. 5, pp. 2537–2546, Oct 2018.
- [16] Y. Miyazaki, "Deployable techniques for small satellites," *Proc. IEEE*, vol. 106, no. 3, pp. 471–483, March 2018.
- [17] H. Oh and T. Park, "Experimental feasibility study of concentrating photovoltaic power system for cubesat applications," *IEEE Trans. Aerosp. Electron. Syst.*, vol. 51, no. 3, pp. 1942–1949, July 2015.
- [18] A. Ali, A. Massoud, M. O. Hasna, T. Khattab, T. Jabban, and M. Aref Nema, "Modeling of cubesat orientation scenario and solar cells for internet of space provision," in *Proc. 9th Int. Conf. Recent Adv. Space Tech. (RAST)*, 2019, pp. 541–546.

- [19] A. Cortiella, D. Vidal, J. Jané, E. Juan, R. Olivé, A. Amézaga, J. F. Muñoz, P. V. H. Carreno-Luengo, and A. Camps, “3cat-2: Attitude determination and control system for a gnss-r earth observation 6u cubesat mission,” *European Journal of Remote Sensing*, vol. 49, no. 1, pp. 759–776, 2016.
- [20] H. Abdelwahab, M. Nawari, and H. Abdalla, “Maximizing solar energy input for cubesat using sun tracking system and a maximum power point tracking,” in *Proc. Int. Conf. Comm. Contr. Comp. Electron. Eng. (ICCCCEE)*, 2017, pp. 1–7.
- [21] R. Al-Ali, “Hybrid Energy Storage System for CubeSat Applications,” Master’s thesis, Khalifa University, Abu Dhabi, United Arab Emirates, 2020.
- [22] M. S. Whittingham, “History, evolution, and future status of energy storage,” *Proc. IEEE*, vol. 100, no. Special Centennial Issue, pp. 1518–1534, 2012.
- [23] X. Wang, Y. Sone, and S. Kuwajima, “Effect of operation conditions on simulated low-earth orbit cycle-life testing of commercial lithium-ion polymer cells,” *J. Power Sources*, vol. 142, no. 1, pp. 313 – 322, 2005.
- [24] K. B. Chin, M. C. Smart, E. J. Brandon, G. S. Bolotin, and N. K. Palmer, “Li-ion battery and supercapacitor hybrid energy system for low temperature smallsat applications,” in *Proc. 28th Annu AIAA/USU Conf. Small Satellites*, August 2014.
- [25] M. Alkali, M. Y. Edries, and A. R. Khan, “Design Considerations and Ground Testing of Electric Double-Layer Capacitors as Energy Storage Components for Nanosatellites,” *J. Small Satellites*, vol. 4, no. 2, pp. 387–405, 2015.
- [26] K. B. Chin, E. J. Brandon, R. V. Bugga, M. C. Smart, S. C. Jones, F. C. Krause, W. C. West, and G. G. Bolotin, “Energy storage technologies for small satellite applications,” *Proc. IEEE*, vol. 106, no. 3, pp. 419–428, March 2018.
- [27] GomSpace, “NanoPower P31u,” 2021. [Online]. Available: <https://gomspace.com/shop/subsystems/power/nanopower-p31u.aspx>
- [28] ——, “NanoPower P80,” 2021. [Online]. Available: <https://gomspace.com/shop/subsystems/power/nanopower-p80.aspx>
- [29] Crystalspace, “P1U “Vasik” Power Supply,” 2021. [Online]. Available: <https://crystalspace.eu/products/crystalspace-p1u-vasik-power-supply/>
- [30] ClydeSpace, “AAC Clyde Space STARBUCK,” 2021. [Online]. Available: [https://www.aac-clyde.space/assets/000/000/188/AAC\\_DataSheet\\_Starbuck-Nano\\_original.pdf?1600342009](https://www.aac-clyde.space/assets/000/000/188/AAC_DataSheet_Starbuck-Nano_original.pdf?1600342009)
- [31] Nanoavionics, “Cubesat Electric Power System,” 2021. [Online]. Available: <https://nanoavionics.com/cubesat-components/cubesat-electrical-power-system-eps/>
- [32] G. Farahani and M. Taherbaneh, “Extracting best reliable scheme for electrical power subsystem (eps) of satellite,” in *Proc. 8th Int. Conf. Recent Adv. Space Tech. (RAST)*, June 2011, pp. 532–537.
- [33] C. S. Clark and A. Mazaras, “Power system challenges for small satellite missions,” in *Proc. Euro. Small Satellite Serv. Symp.*, September 2006.
- [34] O. Shekoofa and E. Kosari, “Comparing the topologies of satellite electrical power subsystem based on system level specifications,” in *Proc. 6th Int. Conf. Recent Adv. Space Tech. (RAST)*, June 2013, pp. 671–675.
- [35] A. Eduganti, V. Khadkikar, H. Zeineldin, M. S. El Moursi, and M. Al Hosani, “Comparison of peak power tracking based electric power system architectures for cubesats,” *IEEE Transactions on Industry Applications*, vol. 57, no. 3, pp. 2758–2768, 2021.
- [36] P. Thirion, “Design and Implementation of On-board Electrical Power Supply of Student Nanosatellite OUFTI-1 of University of Liège,” Master’s thesis, University of Liège, Liège, Belgium, 2009.
- [37] J. Schaffner and J. Puig-Suari, “The Electronic System Design, Analysis, Integration, and Construction of the Cal Poly State University CP1 CubeSat,” in *Proc. 16th Annu AIAA/USU Conf. Small Satellites*, August 2002, pp. 1–12.
- [38] A. Voborník, I. Vertat, and R. Linhart, “Experimental electric power system for small satellites with independent supply channels,” in *Proc. Int. Conf. Appl. Electron. (AE)*, Sep. 2018, pp. 1–7.
- [39] S. Sanchez-Sanjuan1, J. Gonzalez-Llorente1, and R. Hurtado-Velasco1, “Comparison of the incident solar energy and battery storage in a 3u cubesat satellite for different orientation scenarios,” *J. Aerosp. Technol. Manag.*, vol. 8, no. 1, pp. 91–102, Jan-Mar 2016.
- [40] T. Aburouk, S. Kim, H. Masui, and M. Cho, “Design, fabrication, and testing of an electrical double-layer capacitor-based 1u cubesat electrical power system,” *J. Small Satellites*, vol. 7, no. 1, pp. 701–717, 2018.
- [41] T. M. Lim, A. M. Cramer, J. E. Lumpp, and S. A. Rawashdeh, “A modular electrical power system architecture for small spacecraft,” *IEEE Trans. Aerosp. Electron. Syst.*, vol. 54, no. 4, pp. 1832–1849, Aug 2018.
- [42] A. W. Flath, A. M. Cramer, and J. E. Lumpp, “Mathematical programming based approach to modular electric power system design,” in *Proc. IEEE Aero. Conf.*, March 2019, pp. 1–8.
- [43] M. B. et al., “GOLIAT Space Mission: Earth Observation and Near Earth Environment Monitoring Using NanoSatellites,” in *Proc. IAC B4 Small Sat. Mis. Symp.*, 2009, pp. 1–1.
- [44] M. Long, A. Lorenz, G. Rodgers, E. Tapiro, G. Tran, K. Jackson, and R. Twiggs, “A cubesat derived design for a unique academic research mission in earthquake signature detection,” in *Proc. 16th Annu AIAA/USU Conf. Small Satellites*, August 2002, pp. 1–17.
- [45] A. Yusuf and G. S. Prabowo, “Bench model design of the electrical power system for inusat-1 nanosatellite,” in *Proc. Int. Conf. Comm. Net. Sat.(ComNetSat)*, July 2012, pp. 182–186.
- [46] G. M. Marcelino, S. Vega-Martinez, L. O. Seman, L. Kessler Slongo, and E. A. Bezerra, “A critical embedded system challenge: The floripasat-1 mission,” *IEEE Latin America Transactions*, vol. 18, no. 02, pp. 249–256, 2020.
- [47] Y. K. Chen, Y. C. Lai, W. C. Lu, and A. Lin, “Design and implementation of high reliability electrical power system for 2u nutsat,” *IEEE Trans. Aerosp. Electron. Syst.*, pp. 1–1, 2020.
- [48] D. Del Corso, C. Passerone, L. Reyneri, C. Sansoe, S. Speretta, and M. Tranchero, “Design of a university nano-satellite: the picpot case,” *IEEE Trans. Aerosp. Electron. Syst.*, vol. 47, no. 3, pp. 1985–2007, July 2011.
- [49] R. Darbali-Zamora, N. Cobo-Yepes, J. E. Salazar-Duque, E. I. Ortiz-Rivera, and A. A. Rincon-Charris, “Buck converter and sepic based electronic power supply design with mppt and voltage regulation for small satellite applications,” in *Proc. IEEE 44th Photov. Spec. Conf. (PVSC)*, June 2017, pp. 2963–2968.
- [50] J. LaBerteaux, J. Moesta, and B. Bernard, “Advanced Picosatellite Experiment,” *IEEE Aerosp. Electron. Syst. Mag.*, vol. 24, no. 9, pp. 4–9, Sep. 2009.
- [51] L. Peng, Z. Jun, Y. Xiaozhou, and C. Luping, “Design and validation of modular mppt electric power system for multi-u cubesat,” in *Proc. 3rd IEEE Int. Conf. Contr. Sci. Syst. Eng. (ICCSSE)*, Aug 2017, pp. 374–377.
- [52] L. Peng, Z. Jun, and Y. Xiaozhou, “Design and on-orbit verification of eps for the world’s first 12u polarized light detection cubesat,” *Int. J. Aeronaut. Space Sci.*, vol. 19, no. 4, p. 718–729, September 2018.
- [53] J. Bester, B. Groenewald, and R. Wilkinson, “Electrical power system for a 3u cubesat nanosatellite incorporating peak power tracking with dual redundant control,” *Przeglad Elektrotechniczny (Electrical Review)*, vol. 88, no. 4a, pp. 300–304, 2012.
- [54] S. Acharya, F. Alshehhi, A. Tsoupos, O. Khan, M. Elmoursi, V. Khadkikar, H. Zeineldin, and M. Al Hosani, “Modeling and design of electrical power subsystem for cubesats,” in *Proc. Int. Conf. Smart Ener. Syst. Tech. (SEST)*, Sep. 2019, pp. 1–6.
- [55] F. Bagheroskouei, S. Karbasian, M. Baghban, and R. Amjadifard, “Design and implementation of the electrical power subsystem for a small satellite,” in *Proc. 8th Int. Conf. Recent Adv. Space Tech. (RAST)*, June 2017, pp. 209–214.
- [56] L. Maciulis and V. Buzas, “Lituanicasat-2: Design of the 3u in-orbit technology demonstration cubesat,” *IEEE Aerosp. Electron. Syst. Mag.*, vol. 32, no. 6, pp. 34–45, June 2017.
- [57] B. Neji, C. Hamrouni, A. M. Alimi, H. Nakajima, and A. R. Alim, “Hierarchical fuzzy-logic-based electrical power subsystem for pico satellite erpsat-1,” *IEEE Syst. J.*, vol. 9, no. 2, pp. 474–486, June 2015.
- [58] J. Gonzalez-Llorente, D. Rodriguez-Duarte, S. Sanchez-Sanjuan, and A. Rambal-Vecino, “Improving the efficiency of 3u cubesat eps by selecting operating conditions for power converters,” in *Proc. IEEE Aero. Conf.*, March 2015, pp. 1–7.
- [59] A. Slavinskis, M. Pajusalu, H. Kuuste, E. Ilbis, T. Eenmäe, I. Sünter, K. Laizans, H. Ehrrpais, P. Lilias, E. Kulju, J. Viru, J. Kalde, U. Kvell, J. Kütt, K. Zalite, K. Kahn, S. Lätt, J. Envall, P. Toivanen, J. Polkko, P. Janhunen, R. Rosta, T. Kalvas, R. Vendt, V. Allik, and M. Noormaa, “Estcube-1 in-orbit experience and lessons learned,” *IEEE Aerosp. Electron. Syst. Mag.*, vol. 30, no. 8, pp. 12–22, Aug 2015.
- [60] K. Sukumar, K. Kinger, T. John, A. Dev, and K. Shashank, “Adaptive fault tolerant architecture for enhanced reliability of small satellites,” in *Proc. IEEE Aero. Conf.*, March 2016, pp. 1–7.
- [61] T. Piovesan, H. C. Sartori, J. E. Baggio, and J. R. Pinheiro, “Cubesat electrical power supplies optimization — comparison between conventional and optimal design methodology,” in *Proc. 12th IEEE Int. Conf. Ind. Appl. (INDUSCON)*, Nov 2016, pp. 1–7.

- [62] J. A. Carrasco, F. G. de Quirós, H. Alavés, and M. Navalón, "An analog maximum power point tracker with pulsedwidth modulator multiplication for a solar array regulator," *IEEE Trans. Power Electron.*, vol. 34, no. 9, pp. 8808–8815, Sep. 2019.
- [63] D. Selcan, G. Kirbis, and I. Kramberger, "Analog maximum power point tracking for spacecraft within a low earth orbit," *IEEE Trans. Aerosp. Electron. Syst.*, vol. 52, no. 1, pp. 368–378, February 2016.
- [64] S. Corpino and F. Stesina, "Verification of a cubesat via hardware-in-the-loop simulation," *IEEE Trans. Aerosp. Electron. Syst.*, vol. 50, no. 4, pp. 2807–2818, October 2014.
- [65] S. Dahbi, A. Aziz, S. Zouggar, N. Benazzi, H. Zahboune, and M. Elhafyani, "Design and sizing of electrical power source for a nanosatellite using photovoltaic cells," in *Proc. 3rd Int. Ren. Sust. Ener. Conf. (IRSEC)*, Dec 2015, pp. 1–6.
- [66] P. K. Peter and V. Agarwal, "Switched capacitor dc-dc converter based maximum power point tracking of a pv source for nano satellite application," in *Proc. 35th IEEE Photovoltaic Spec. Conf.*, June 2010, pp. 002604–002609.
- [67] P. S. Padma, A. Radhika, and V. T. Deepika, "Mppt and sepic based controller development for energy utilisation in cubesats," in *Proc. Annual IEEE India Conf. (INDICON)*, 2012, pp. 143–148.
- [68] R. Darbali-Zamora, D. Merced-Cirino, J. Rivera-Alamo, E. I. Ortiz-Rivera, and A. A. Rincon-Charris, "Design and thermal testing of a power supply prototype for the space plasma ionic charge analyzer (spica) cubesat," in *Proc. IEEE 42nd Photov. Spec. Conf. (PVSC)*, 2015, pp. 1–6.
- [69] J. Wells, L. Stras, and T. Jeans, "Canada's smallest satellite: The canadian advanced nanospace experiment (canx-1)," in *Proc. 16th Annu AIAA/USU Conf. Small Satellites*, August 2002.
- [70] Å. Riise, B. Samuelsen, N. Sokolova, H. D. Cederblad, J. Fasselstad, C. Nordin, E. Sæther, J. Otterstad, K. M. Fauske, O. K. Eriksen, F. M. Indergaard, K. Svartveit, and P. E. Furebotten, "ncube: The first norwegian student satellite," in *Proc. 17th Annu AIAA/USU Conf. Small Satellites*, August 2003, pp. 1–12.
- [71] A. Eduganti, V. Khadkikar, M. S. Elmoursi, H. Zeineldin, and M. Al Hosani, "A novel eps architecture for 1u/2u cubesats with enhanced fault-tolerant capability," in *2020 IEEE Industry Applications Society Annual Meeting*, 2020, pp. 1–6.
- [72] S. Kulkarni, S. Bangade, M. Khadse, D. Waghulde, P. Aher, K. Gaikwad, and S. Thakurdesai, "Design and optimization of the on board DC/DC converters of Swayam satellite," in *Proc. IEEE Int. Conf. Power Electron. Drives Energy Syst. (PEDES)*, Dec 2014, pp. 1–6.
- [73] R. Joshi, S. Kulkarni, S. Bangade, A. Thusé, P. Hegde, P. Wakde, and S. Krishnakumar, "A Modular, Efficient, Low Cost Power System For Pico-Satellite Applications," in *Proc. Int. Astro. Cong. (IAC-12)*, October 2012, pp. 1–6.
- [74] A. Davidson, "Cubesat hybrid energy storage architecture (hesa)," 2017. [Online]. Available: [https://ibeos.com/documents/cubesat/Cubic\\_CubeSat\\_HESS.pdf](https://ibeos.com/documents/cubesat/Cubic_CubeSat_HESS.pdf)
- [75] M. Obland, D. M. Klumpar, S. Kirn, G. Hunyadi, S. Jepsen, and B. Larsen, "Power subsystem design for the Montana EaRth Orbiting Pico-Explorer (MEROPE) CubeSat-class satellite," in *Proc. IEEE Aero. Conf.*, vol. 1, March 2002, pp. 1–1.
- [76] G. Bonin, D. Sinclair, and R. Zee, "Peak power tracking on a nanosatellite scale: The design and implementation of digital power electronics on the sfl generic nanosatellite bus," in *Proc. 23rd Annu AIAA/USU Conf. on Small Satellites*, August 2009.
- [77] S. A. Kimura, H. Wijanto, Edwar, F. F. Arribat Rafsanzani, H. Prananditiya, and A. A. Ichwan, "Development of the electronic power subsystem design for tel-usat," in *Proc. IEEE Int. Conf. Sig. Syst. (ICSigSys)*, July 2019, pp. 120–125.
- [78] A. Davidson, "150-Watt SmallSat Electric Power System," 2019. [Online]. Available: [https://ibeos.com/documents/cubesat/Ibeos\\_CubeSat\\_EPS.pdf](https://ibeos.com/documents/cubesat/Ibeos_CubeSat_EPS.pdf)
- [79] B. Lynch and C. Wallace, "CubeSat electronic power system," Santa Clara, California, US, June 2013.
- [80] V. Pooler, E. Priidel, and V. Sinivee, "Reliable smart electrical power supply for cubesat platforms," in *2016 15th Biennial Baltic Electron. Conf. (BEC)*, Oct 2016, pp. 215–218.
- [81] H. Ashida, K. Fujihashi, S. Inagawa, Y. Miura, K. Omagari, N. Miyashita, S. Matunaga, T. Toizumi, J. Kataoka, and N. Kawai, "Design of tokyo tech nano-satellite cute-1.7+apd ii and its operation," *Acta Astronautica*, vol. 66, no. 9, pp. 1412 – 1424, 2010.
- [82] Cute-1.7 EPS, "Cute-1.7 + APD - Sub Systems." [Online]. Available: [http://lss.mes.titech.ac.jp/ssp/cute1.7/cute1.7-1/subsystem\\_eps\\_e.html](http://lss.mes.titech.ac.jp/ssp/cute1.7/cute1.7-1/subsystem_eps_e.html).
- [83] S. Gopakumar, S. Eega, S. V. S. Suresh, M. S. S. Reddy, A. Antony, H. Ramachandran, and D. Koilpillai, "Design of electrical power subsystem for iitsatsat," in *Proc. Int. Conf. Space Sci. Commu. (IconSpace)*, Aug 2015, pp. 175–180.
- [84] M. Kompella, R. S. Kaarthik, H. Priyadarshnam, and H. S. M.S., "Parallel operation of battery chargers in small satellite electrical power systems," in *IEEE 16th India Coun. Int. Conf. (INDICON)*, Dec 2019, pp. 1–4.
- [85] S. Notani and S. Bhattacharya, "Flexible electrical power system controller design and battery integration for 1u to 12u cubesats," in *Proc. IEEE Ener. Conv. Cong. Expo.*, Sep. 2011, pp. 3633–3640.
- [86] M. Shah, A. Juneja, S. Bhattacharya, and A. G. Dean, "High frequency gan device-enabled cubesat eps with real-time scheduling," in *Proc. IEEE Ener. Conv. Cong. Expo. (ECCE)*, Sep. 2012, pp. 2934–2941.
- [87] S. Singh, A. Shrivastav, and S. Bhattacharya, "Gan fet based cubesat electrical power system," in *Proc. IEEE Appl. Power Electron. Conf. Expo.(APEC)*, March 2015, pp. 1388–1395.
- [88] A. Shrivastav, S. Singh, A. Mahajan, and S. Bhattacharya, "Effective control software techniques for high efficiency gan fet based flexible electrical power system for cube-satellites," in *Proc. IEEE Appl. Power Electron. Conf. Expo. (APEC)*, 2016, pp. 601–608.
- [89] E. Mattos, A. M. S. S. Andrade, G. V. Hollweg, M. L. da S. Martins, and J. R. Pinheiro, "Analysis and design of a stacked power subsystem on a picosatellite," *IEEE Aerosp. Electron. Syst. Mag.*, vol. 33, no. 10, pp. 4–13, Oct 2018.
- [90] V. Thakurta, V. Datla, A. Ravi, R. Reddy, A. Jain, A. Akhoury, A. Parashar, H. Dali, and A. Kejriwal, "Design and implementation of power management algorithm for a nano-satellite," in *Proc. IEEE Aero. Conf.*, March 2019, pp. 1–11.
- [91] O. Khan, M. Elmoursi, H. Zeineldin, V. Khadkikar, and M. Al Hosani, "Benchmark model for multi-orbital transient analysis of satellite electrical power subsystem," *IET Ren. Power Gen.*, vol. 14, pp. 286–296(10), February 2020. [Online]. Available: <https://digital-library.theiet.org/content/journals/10.1049/iet-rpg.2019.1102>
- [92] K. M. Hegde, A. C.R., A. K., and P. Kashyap, "Design and development of rvsat-1, a student nano-satellite with biological payload," in *2019 IEEE Aerospace Conference*, March 2019, pp. 1–14.
- [93] A. Lashab, M. Yaqoob, Y. Terriche, J. C. Vasquez, and J. M. Guerrero, "Space microgrids: New concepts on electric power systems for satellites," *IEEE Electr. Mag.*, vol. 8, no. 4, pp. 8–19, 2020.
- [94] P. T. Huynh and B. H. Cho, "Design and analysis of a regulated peak-power tracking system," *IEEE Trans. Aerosp. Electron. Syst.*, vol. 35, no. 1, pp. 84–92, Jan 1999.
- [95] R. Burt, "Distributed Electrical Power System in Cubesat Applications," Master's thesis, Utah State University, Logan, Utah, US, 2011.
- [96] O. Khan, M. Elmoursi, H. Zeineldin, V. Khadkikar, and M. Al Hosani, "A comprehensive design and control methodology for dc-powered satellite electrical subsystem based on pv and battery," *IET Ren. Power Gen.*, p. Accepted, 2020.
- [97] O. Garcia, P. Alou, J. A. Oliver, D. Diaz, D. Meneses, J. A. Cobos, A. Soto, E. Lapena, and J. Rancano, "Comparison of boost-based mppt topologies for space applications," *IEEE Trans. Aerosp. Electron. Syst.*, vol. 49, no. 2, pp. 1091–1107, APRIL 2013.
- [98] M. Mughal, "Student research highlight smart panel bodies for modular small satellites," *IEEE Aerosp. Electron. Syst. Mag.*, vol. 29, no. 12, pp. 38–41, Dec 2014.
- [99] M. Chen, K. K. Afridi, S. Chakraborty, and D. J. Perreault, "Multitrack power conversion architecture," *IEEE Trans. Power Electron.*, vol. 32, no. 1, pp. 325–340, Jan 2017.
- [100] M. Uno and A. Kukita, "Multi-port converter integrating boost and switched capacitor converters for single-cell battery power system in small satellite," in *Proc. IEEE ECCE Asia Downunder*, 2013, pp. 747–752.
- [101] —, "Pwm converter integrating switched capacitor converter and series-resonant voltage multiplier as equalizers for photovoltaic modules and series-connected energy storage cells for exploration rovers," *IEEE Transactions on Power Electronics*, vol. 32, no. 11, pp. 8500–8513, Nov 2017.
- [102] M. Langer and J. Bouwmeester, "Reliability of cubesats statistical data, developers beliefs and the way forward," in *Proc. 30th Annu AIAA/USU Conf. Small Satellites*, July 2016.
- [103] M. Pecht and A. Dasgupta, "Physics-of-failure: an approach to reliable product development," in *IEEE 1995 International Integrated Reliability Workshop. Final Report*, Oct 1995, pp. 1–4.
- [104] H. Kimm and M. Jarrell, "Controller area network for fault tolerant small satellite system design," in *Proc. 2014 IEEE 23rd Int. Sym. Ind. Electron.*, June 2014, pp. 81–86.

- [105] X. Luo, Y. Wang, Y. Hao, X. Li, C. Liu, X. Fei, C. Yu, and F. Cao, "Research of single-event burnout and hardening of algan/gan-based misfet," *IEEE Trans. Electron Devices*, vol. 66, no. 2, pp. 1118–1122, Feb 2019.
- [106] A. K. Bhattacharjee, N. Kutkut, and I. Batarseh, "Review of multiport converters for solar and energy storage integration," *IEEE Trans. Power Electron.*, vol. 34, no. 2, pp. 1431–1445, Feb 2019.
- [107] Yaow-Ming Chen, Yuan-Chuan Liu, and Feng-Yu Wu, "Multi-input dc/dc converter based on the multiwinding transformer for renewable energy applications," *IEEE Trans. Ind. Appl.*, vol. 38, no. 4, pp. 1096–1104, July 2002.
- [108] S. Athikkal, G. Guru Kumar, K. Sundaramoorthy, and A. Sankar, "A non-isolated bridge-type dc–dc converter for hybrid energy source integration," *IEEE Trans. Ind. Appl.*, vol. 55, no. 4, pp. 4033–4043, July 2019.
- [109] H. Krishnaswami and N. Mohan, "Three-port series-resonant dc–dc converter to interface renewable energy sources with bidirectional load and energy storage ports," *IEEE Trans. Power Electron.*, vol. 24, no. 10, pp. 2289–2297, 2009.
- [110] Z. Qian, O. Abdel-Rahman, H. Al-Atrash, and I. Batarseh, "Modeling and control of three-port dc/dc converter interface for satellite applications," *IEEE Trans. Power Electron.*, vol. 25, no. 3, pp. 637–649, March 2010.
- [111] Z. Qian, O. Abdel-Rahman, H. Hu, and I. Batarseh, "Multi-channel three-port dc/dc converters as maximum power tracker, battery charger and bus regulator," in *Proc. IEEE Appl. Power Electron. Conf. Expo. (APEC)*, 2010, pp. 2073–2079.
- [112] Z. Qian, O. Abdel-Rahman, K. Zhang, H. Hu, J. Shen, and I. Batarseh, "Design and analysis of three-port dc/dc converters for satellite platform power system," in *Proc. IEEE Energy Conversion Congress and Expo.*, 2011, pp. 1454–1460.
- [113] J. Zhang, H. Wu, Y. Xing, H. Hu, and F. Cao, "Power management of a modular three-port converter-based spacecraft power system," *IEEE Trans. Aerosp. Electron. Syst.*, vol. 52, no. 1, pp. 486–492, February 2016.
- [114] M. Di and Z. Naitong, "A novel multiple-port converter for high power satellite platform," in *Proc. Int. Conf. Mechatron. Sci. Elect. Eng. Comp. (MEC)*, 2013, pp. 3030–3036.
- [115] O. Mourra, A. Fernandez, F. Tonicello, and S. Landstroem, "Multiple port dc dc converter for spacecraft power conditioning unit," in *Proc. IEEE Appl. Power Electron. Conf. Expo. (APEC)*, Feb 2012, pp. 1278–1285.
- [116] F. Li, X. You, and Y. Li, "Design of a multi-port converter using dual-frequency pwm control for satellite applications," in *Proc. IEEE Appl. Power Electron. Conf. Expo. (APEC)*, March 2014, pp. 1178–1184.
- [117] W. Imes and F. Rodriguez, "A two-input tri-state converter for spacecraft power conditioning," in *Proc. Intersociety Energy Convers. Eng. Conf.*, Aug 1994.
- [118] H. Nagata and M. Uno, "Nonisolated pwm three-port converter realizing reduced circuit volume for satellite electrical power systems," *IEEE Trans. Aerosp. Electron. Syst.*, vol. 56, no. 5, pp. 3394–3408, 2020.
- [119] M. Uno and K. Sugiyama, "Switched capacitor converter based multiport converter integrating bidirectional pwm and series-resonant converters for standalone photovoltaic systems," *IEEE Transactions on Power Electronics*, vol. 34, no. 2, pp. 1394–1406, Feb 2019.
- [120] T. Rahimi, L. Ding, R. Faraji, M. Kheshti, J. Pou, and K. H. Loo, "Performance analyses of a three-port converter for post-fault conditions in aerospace applications," in *Proc. 12th Power Electron. Drive Sys. Tech. Conf. (PEDSTC)*, 2021, pp. 1–6.
- [121] H. Wu, K. Sun, S. Ding, and Y. Xing, "Topology derivation of nonisolated three-port dc–dc converters from dic and doc," *IEEE Transactions on Power Electronics*, vol. 28, no. 7, pp. 3297–3307, 2013.
- [122] S. Jin, D. Zhang, C. Wang, and Y. Gu, "Optimized design of space solar array simulator with novel three-port linear power composite transistor based on multiple cascaded sic-jfets," *IEEE Trans. Ind. Electron.*, vol. 65, no. 6, pp. 4691–4701, 2018.
- [123] Q. Tian, G. Zhou, R. Liu, X. Zhang, and M. Leng, "Topology synthesis of a family of integrated three-port converters for renewable energy system applications," *IEEE Trans. Ind. Electron.*, vol. 68, no. 7, pp. 5833–5846, July 2021.
- [124] A. Edpuganti, V. Khadkikar, M. S. Elmoursi, and H. Zeineldin, "A novel multiport converter interface for solar panels of cubesat," *IEEE Trans. Power Electron.*, pp. 1–15, 2021.
- [125] M. Kasper, D. Bortis, and J. W. Kolar, "Classification and comparative evaluation of pv panel-integrated dc–dc converter concepts," *IEEE Trans. Power Electron.*, vol. 29, no. 5, pp. 2511–2526, May 2014.



**Amarendra Edpuganti** (S'14–M'16) received the B.Tech. degree in electrical and electronics engineering from the National Institute of Technology, Warangal, India, in 2007, the M.Tech degree in electrical engineering from the Indian Institute of Technology, Kanpur, India, in 2012, and the Ph.D. degree in electrical and computer engineering from the National University of Singapore, Singapore, in 2016. He was a Software Engineer with Adobe Systems Inc., Bangalore, India, from August 2007 to December 2009. He worked as an R&D Engineer with the Grid Systems R&D, ABB Global Industries and Services Pvt Ltd., Chennai, India, from October 2015 to July 2018. He is currently a Postdoctoral Fellow with Khalifa University, Abu Dhabi, UAE. His research interests include power electronics applications in spacecraft power systems, medium-voltage drives, high-voltage dc transmission systems, renewable energy integration, and electric vehicles.



**Vinod Khadkikar** (S'06, M'09, SM'15) received the M. Tech. in power electronics, electrical machines, and drives from the Indian Institute of Technology (IITD), New Delhi, India, in 2002 and the Ph.D. degree in electrical engineering from the École de Technologie Supérieure, Montréal, QC, Canada, in 2008. From December 2008 to March 2010, he was a Postdoctoral Fellow at the University of Western Ontario, London, ON, Canada. In 2010, he was a Visiting Faculty at the Massachusetts Institute of Technology (MIT), Cambridge, MA, USA. He is currently a Professor with the Department of Electrical Engineering and Computer Science, Khalifa University, Abu Dhabi, United Arab Emirates. His research interests include applications of power electronics in distribution systems and renewable energy resources, grid interconnection issues, power quality enhancement, active power filters, and electric vehicles.

Dr. Khadkikar is currently an Associate Editor for the IEEE Transactions on Industrial Electronics, IEEE Transactions on Industry Applications and IET Power Electronics.



**Mohamed Shawky El Moursi** (M'12, SM'15) received the B.Sc. and M.Sc. degrees from Mansoura University, Mansoura, Egypt, in 1997 and 2002, respectively, and the Ph.D. degree from the University of New Brunswick (UNB), Fredericton, NB, Canada, in 2005, all in electrical engineering. He was a Research and Teaching Assistant in the Department of Electrical and Computer Engineering, UNB, from 2002 to 2005. He joined McGill University as a Postdoctoral Fellow with the Power Electronics Group. He joined Vestas Wind Systems, Arhus, Denmark, in the Technology R&D with the Wind Power Plant Group. He was with TRANSCO, UAE, as a Senior Study and Planning Engineer. He is currently a Professor in the Electrical and Computer Engineering Department at Khalifa University of Science and Technology- Masdar Campus and seconded to a Professor Position in the Faculty of Engineering, Mansoura University, Mansoura, Egypt, and currently on leave. He was a Visiting Professor at the Massachusetts Institute of Technology, Cambridge, Massachusetts, USA. Dr. Shawky is currently an Editor of IEEE Transactions on Power Delivery, IEEE Transactions on Power Systems, Associate Editor of IEEE Transactions on Power Electronics, Associate Editor of IEEE Transactions on Smart Grid, Guest Editor of IEEE Transactions on Energy Conversion, Guest Editor-in-Chief for the special section between TPWRD and TPWRS, Editor for IEEE Power Engineering Letters, Regional Editor for IET Renewable Power Generation and Associate Editor for IET Power Electronics Journals. His research interests include power system, power electronics, FACTS technologies, VSC-HVDC systems, Microgrid operation and control, Renewable energy systems (Wind and PV) integration, and interconnections.



**H. H. Zeineldin** (M'06–SM'13) received the B.Sc. and M.Sc. degrees in electrical engineering from Cairo University, Giza, Egypt, in 1999 and 2002, respectively, and the Ph.D. degree in electrical and computer engineering from the University of Waterloo, Waterloo, ON, Canada, in 2006. He was with Smith and Andersen Electrical Engineering, Inc., North York, ON, USA, where he was involved in projects involving distribution system designs, protection, and distributed generation. He was a Visiting Professor with the Massachusetts Institute of Technology, Cambridge, MA, USA. He is with Khalifa University of Science and Technology, Abu Dhabi, UAE and is currently on leave from the Faculty of Engineering, Cairo University, Egypt. His current research interests include distribution system protection, distributed generation, and micro grids. He is currently an Editor for the IEEE TRANSACTIONS ON ENERGY CONVERSION.

of Technology, Cambridge, MA, USA. He is with Khalifa University of Science and Technology, Abu Dhabi, UAE and is currently on leave from the Faculty of Engineering, Cairo University, Egypt. His current research interests include distribution system protection, distributed generation, and micro grids. He is currently an Editor for the IEEE TRANSACTIONS ON ENERGY CONVERSION.



**Naji Al-Sayari** received his BSc degree in Electrical Engineering from Florida Institute of Technology, Florida, USA, MSc in Electrical Engineering from Washington University in St. Louis, Missouri, USA and his PhD from the University of Manchester, Manchester, UK in 2001, 2005 and 2011, respectively. Currently Dr. Al-Sayari is an assistant professor in the Electrical Engineering and Computer Science Department at Khalifa University, Abu Dhabi, UAE. His current research interests includes electric machines analysis, power electronics applications, power quality issues, distributed generation, smart grid, micro-grid and renewable energy systems. He is also the co-founder of the Power Electronics and Advanced Sustainable Energy (PEACE) Lab at Khalifa University.



**Khalifa Al Hosani** (Senior Member, IEEE) received the B.Sc. and M.Sc. degrees in electrical engineering from the University of Notre Dame, Notre Dame, IN, USA, in 2005 and 2007, respectively, and the Ph.D. degree in electrical and computer engineering from The Ohio State University, Columbus, OH, USA, in 2011. He is currently an Associate Professor with the Department of Electrical and Computer Engineering, Khalifa University, Abu Dhabi, United Arab Emirates. He is also an Engineering & Technology affiliate member of Mohammed bin Rashed Academy

of Scientists (MBRAS). He is the Co-Founder of the Power Electronics and Advanced Sustainable Energy Center Laboratory, ADNOC Research and Innovation Center (now Power Electronics and Sustainable Energy (PEASE) Research Lab at Khalifa University) Abu Dhabi, United Arab Emirates. His research interests include a wide range of topics including nonlinear control, sliding mode control, control of power electronics, power systems stability and control, renewable energy systems modeling and control, smart grid, microgrid and distributed generation, and application of control theory to oil and gas applications.